PPU College of Engineering and Technology

The Home of Competent Engineers and Researchers

Mechanical Engineering Department

Automotive Engineering

Bachelor Thesis

Graduation Project

Design Of Mechanisms To prevent Engine Stalling During Take Off And Gear Shifting

Project Team

Hamza Talahmeh

Qutaiba Ghunaim

Abdelnasser Tafesh

Project Supervisor

Dr. Mohammed AlQawasmi

Hebron – Palestine

January, 2013

Abstract

New drivers, drivers with low experience and disabled people are suffering from difficulties such as engine stalling during vehicle take off, gear shifting and choice of unsuitable gear ratio, while driving vehicle with manual gear box.

To overcome these difficulties we will design assistance systems (electronic systems & mechanical system) to help driver to prevent engine stalling in mentioned conditions.

First system: electronic systems which include sensors, switches and microcontroller to overcome engine stalling due to choice of unsuitable gear ratio.

Second system: mechanical system which include pneumatic -chock- absorber that will be added to clutch pedal to overcome engine stalling during vehicle take off and gear shifting.

Table of contents

List of Tables

List of Figures

List of Symbols:

Symbol	Meaning	SI Units
a_1, a_2, b	Constants, length	M
C	Viscous damping coefficient	N.s/m
J_0	Mass moment of inertia	$Kg.m^2$
K	Spring constant	N/m
ξ	Damping ratio	unit less
Θ	Angular displacement	Rad
$\dot{\Theta}$	Angular velocity	Rad/sec
$\ddot{\Theta}$	Angular acceleration	Rad/sec^2
ω_n	Natural frequency	Rad/sec
D	Diameter of chock absorber	M
D	Deflection of chock absorber	M
ρ	Air density	Kg/m^3
H	Length of stroke inside chock absorber	M
m_w	Wire mass	Kg

Chapter One

Introduction

1.1 Overview

Since the lunching of vehicles manufacturing, most vehicles have been used a clutch and a manual transmission recently, Automotive industry manufacture vehicles with automatic transmission, which spread widely and rapidly; because its advantages.

Automatic transmission is more comfort than manual transmission especially for new drivers and disabled people, but despite that, people in less developed countries still prefer vehicles with clutch and manual transmission because of lack of specialized centers for maintenance and repairing of automatic transmission in addition to absence of skilled people in this field.

Driving vehicles with manual transmission need some experience which not exist especially for new drivers and disabled people, these drivers often facing difficulties in driving especially during takeoff and gear shifting which may lead to engine stalling, and in convenience during driving.

1.2 Importance of the project

Automotive designers aimed to increase the level of comfort for drivers while driving, this project provides a great deal of comfort for drivers, especially new drivers and disabled people, when driving vehicles with clutches and manual transmission, where a pneumatic -chock- absorber will be added in clutch applying mechanism to help to engage clutch properly and electronic systems will be designed to help to select suitable gear ratio smoothly according to road requirements and vehicle speed.

The project also aims to reduce traffic jam and rate of accidents caused by stalling engine during takeoff and speeds shifting, this also will decrease fuel consumption and increase service life of clutch and transmission.

1.3 Project Objectives

The main purpose of the project is to design mechanisms to prevent engine stalling during takeoff and gear shifting and choice unsuitable gear ratio. The proposed design contains a mechanical system and an electronic system:

- The mechanical system will include pneumatic -chock- absorber which will be incorporated to clutch pedal to engage clutch gradually during takeoff and gear shifting.

- The electronic systems include assistance mechanism for choosing suitable gear ratio, to warn the driver when choosing unsuitable gear ratio. This electronic system will include vehicle speed sensor, gear position sensor on the gear lever, liquid crystal display and PIC. PIC will send warning when driver choosing unsuitable gear ratio by comparing vehicle speed gear ratio on LCD to make shift up or shift down.

1.4 The budget for the project

Table (1.1) Actual budget table for the project

Task	No.	Cost (NIS)	Total
Car	1	2500	2500
Chock absorber	1	100	100
LCD	1	90	90
Microcontroller (PIC)	1	80	80
Switches	7	10	70
LM2917N	2	50	100
Other electronic parts	-	300	300
Total			3240

1.5 The time planning for the project

The project plan follows the time schedule, which includes the related tasks of study and system analysis. The following time planar for the first semester and second semester.

The time table for the first semester is illustrated in table (1.2).

Table (1.2) First semester time plan:

Task\Week	1	2	3	4	5	6	7	8	9	10	11	12	13	14	15	16
Selecting project title																
Data collection																
Identify function and task																
Design and Analysis																
Documentation																

The time table for the second semester is illustrated in table (1.3):

Table (1.3) second semester time plan:

Task\Week	1	2	3	4	5	6	7	8	9	10	11	12	13	14	15	16
System building																
Write the PIC programming																
Testing																
Installation systems on car																
Documentation																

Chapter Two

Systems components operating principles

2.1 Description of mechanical system

2.1.1 Introduction

Automobiles have many systems for human comfort such as air conditioning system, multimedia system and communication system, and systems for safety such as ABS system, ESP system, TCS system, seat comfort systems, air bags, in addition to that some vehicles has special mechanisms for disabled people, soundproofing the interior of the passenger compartment, active and passive safety systems.

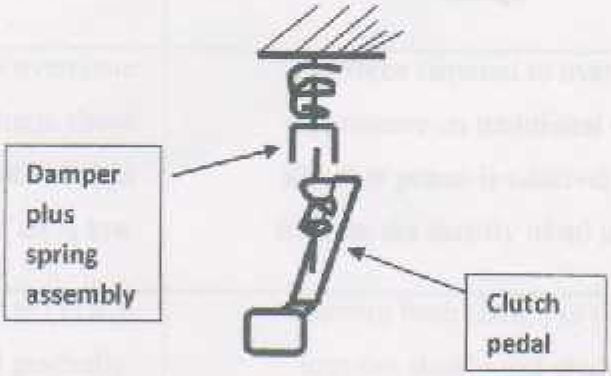

Figure (2-1) Description of mechanical system

In this project the addition design is a mechanical system which helps mainly in return clutch gradually. As shown in figure (2-1) a chock absorber will be added in clutch release mechanism to achieve the mentioned purpose.

2.1.2 Description of chock absorber

There are two main types of - chock - absorbers a pneumatic and traditional - chock - absorber, and table (2.1) show a comparison between the mentioned types of - chock - absorbers. [1]

Table (2.1) comparison between - chock - absorber design types

Pneumatic - chock - absorber design	Traditional - chock- absorber design
The force required to overcome air pressure on pneumatic chock absorber piston is relatively low because the density of air is low.	The force required to overcome oil pressure on traditional chock absorber piston is relatively high because the density of oil is high.
Moving from (BDC) to (TDC) happens quickly and gradually because low viscosity of air.	Moving from (BDC) to (TDC) happens slowly and gradually because high viscosity of oil.
Eliminate increasing of clutch temperature to increase service life of clutch.	Increasing in clutch temperature to decrease service life of clutch.
Relatively low cost.	Relatively high cost.

So, pneumatic -chock- absorber is more suitable to use the better type to use in this mechanism. In general added - chock - absorber work to decreases clutch wear by absorb the shock between flywheel and clutch friction disc ,and prevent engine stalling during takeoff especially for disabled people and new drivers.

2.1.2.1 Description of pneumatic chock absorber

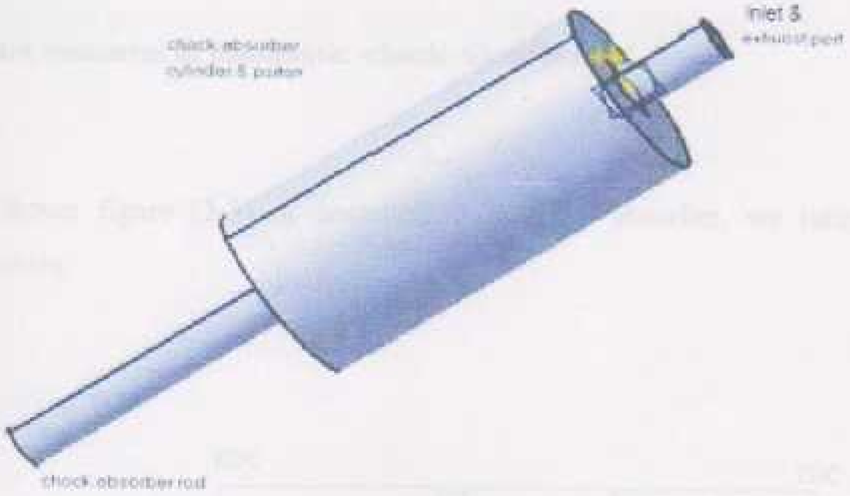

Figure (2-2) pneumatic -chock- absorber designed by Catia

Disengagement period of pneumatic chock absorber

During disengagement period the pneumatic – chock - absorber will be in suction (intake) stroke, atmospheric air moves to pneumatic - chock - absorber cylinder by vacuum. So, rapid clutch disengagement obtained.

Engagement period of pneumatic - chock - absorber

During engagement period the pneumatic -chock- absorber will be in delivery (exhaust) stroke, atmospheric air exit from small pneumatic -chock- absorber-exhaust port. So, rapid gradually clutch engagement obtained.

2.1.2.2 Main measures of pneumatic -chock- absorber

As shown figure (2-3) of pneumatic - chock - absorber, we take some important notes:

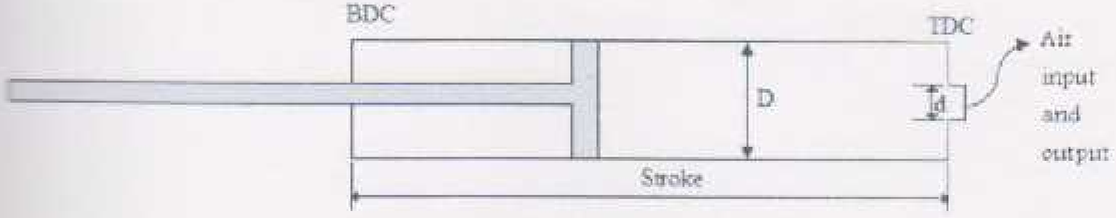

Figure (2-3) Main measures of pneumatic -chock- absorber

1- Stroke is the distance from top dead center (TDC) to bottom dead center (BDC). So, the stroke must be equal to clutch pedal travel from clutch release position to fully clutch applying position.

2- Volume of intake air equal to volume of pneumatic - chock - absorber cylinder.

3- Diameter of exhaust port.

4- Diameter of pneumatic - chock - absorber cylinder.

5- Velocity of pneumatic - chock - absorber piston from (BDC) to (TDC).

2.2 Description of an assistance mechanism for choosing suitable gear ratio

2.2.1 Introduction

Disabled people and new drivers usually suffering during choosing an appropriate gear ratio which suitable for specific vehicle speed and road requirements, so an electronic system will be designed (figure 2-4) which include sensors and switches to help driver for choosing the right gear ratio.

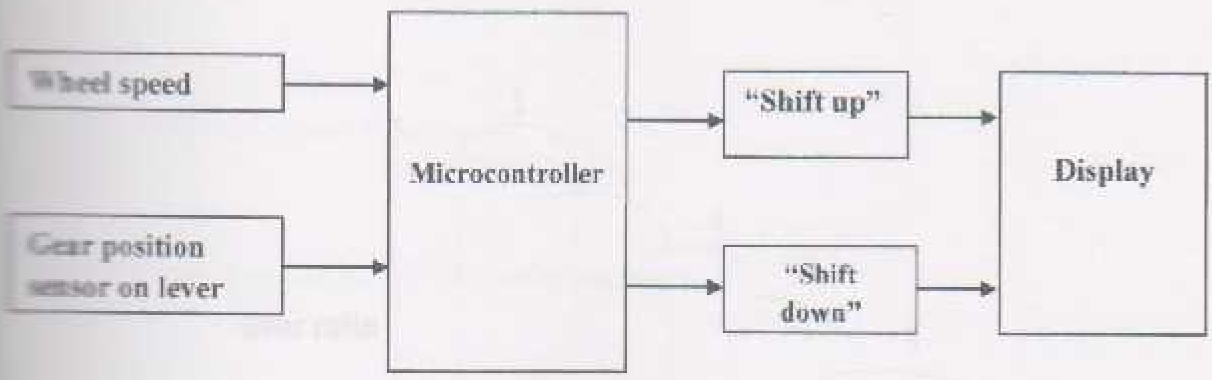

Figure (2-4) Description of mechanical system

Every gear ratio has a range of vehicle speed (figure 2-5), as shown below every gear ratio has speed in Km/h (table 2.2). So when disabled people or a new driver choosing unsuitable gear ratio the engine may stall or will operate very poor.

Table (2.2) Gear ratio and the vehicle speed ranges relationship

Gear Number	Vehicle Speed Range (Km/h)
1	0-20
2	20-40
3	40-60
4	60-140
5	140-200

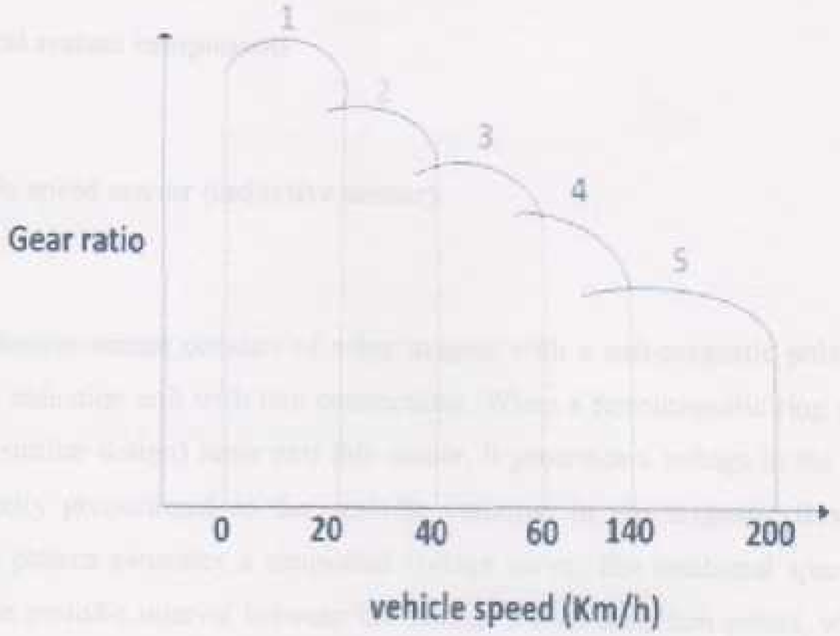

Figure (2-5) The relationship between vehicle speed and gear ratios [2]

To solve this problem an electronic system will be designed to assist in choosing suitable gear ratio which will work in two stages: first-stage is comparing and analyzing stage; second-stage is warning stage.

Table (2.3) electronic system stages and its goals

Electronic system stages	The goal
comparing stage	Compare between 2-inputs at PIC
Print on LCD stage	Send output to LCD by PIC

2.2.2 Electrical system components

2.2.2.1 Vehicle speed sensor (inductive sensor)

The inductive sensor consists of a bar magnet with a soft-magnetic pole pin supporting an induction coil with two connections. When a ferromagnetic ring gear (or a rotor of similar design) turns past this sensor, it generates a voltage in the coil which is directly proportional to the periodic variation in the magnetic flux. A uniform tooth pattern generates a sinusoidal voltage curve. The rotational speed is reflected in the periodic interval between the voltage's zero transition points, while the amplitude is also proportional to rotating speed. The air gap and the tooth dimensions are vital factors in defining the (exponential) signal amplitude. Teeth can still be detected without difficulty up to air-gap widths of one half or one third of a tooth interval. Standard gears for crankshaft and ABS wheel-speed sensors cover gaps ranging from 0.8 to 1.5 mm. The reference point for the ignition timing is obtained either by omitting a tooth or by bridging a gap between teeth. The resulting increase in distance between zero transitions is identified as the reference point and is accompanied by a substantial increase in signal voltage (the system registers a larger tooth.) [3].

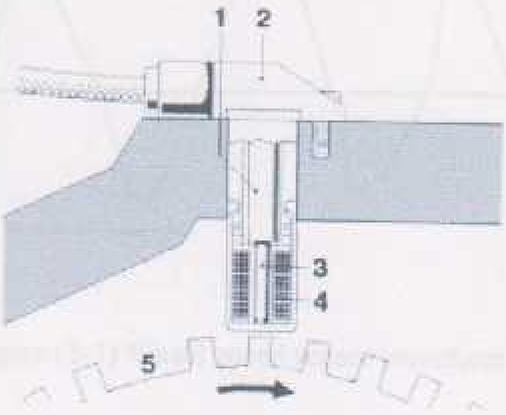

Figure (2-6) Inductive sensor

1- Permanent magnet 2- Housing 3- Soft irons Core 4- winding

5- Ring gear (iron) with reference point.

Speed sensor will produce an output signal that can be monitored and measured on the oscilloscope. Figure (2-7)

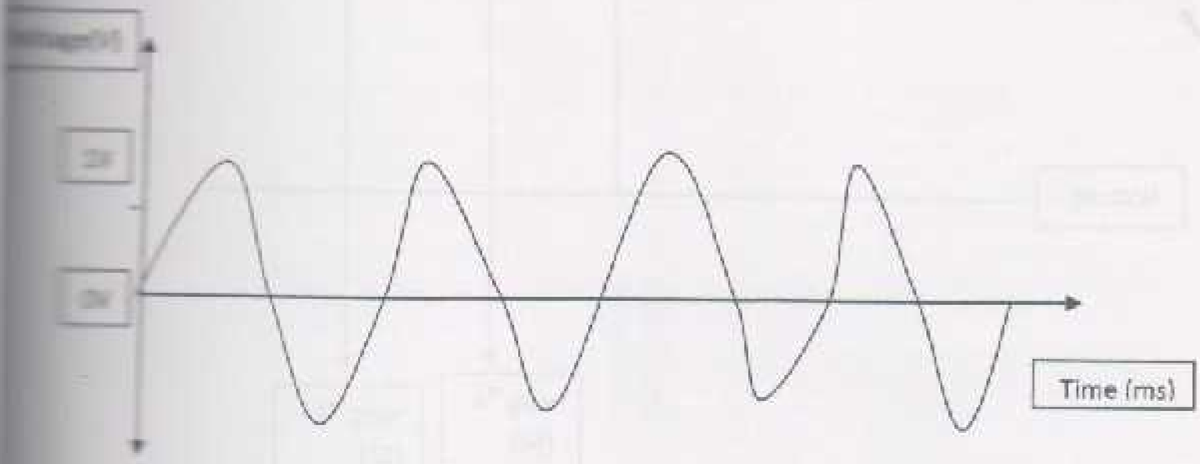

Figure (2-7) Wheel speed sensor waveform [4]

2.2.2.2 Gear position sensor

Switches have been used to determine gear position and produce input signal to microcontroller, the structure of switches from table (2.4) and figure (2-8).

Table (2.4): switches numbers and gear position

Switch number	Gear position
S1	1st gear
S2	2nd gear
S3	3rd gear
S4	4th gear
S5	5th gear

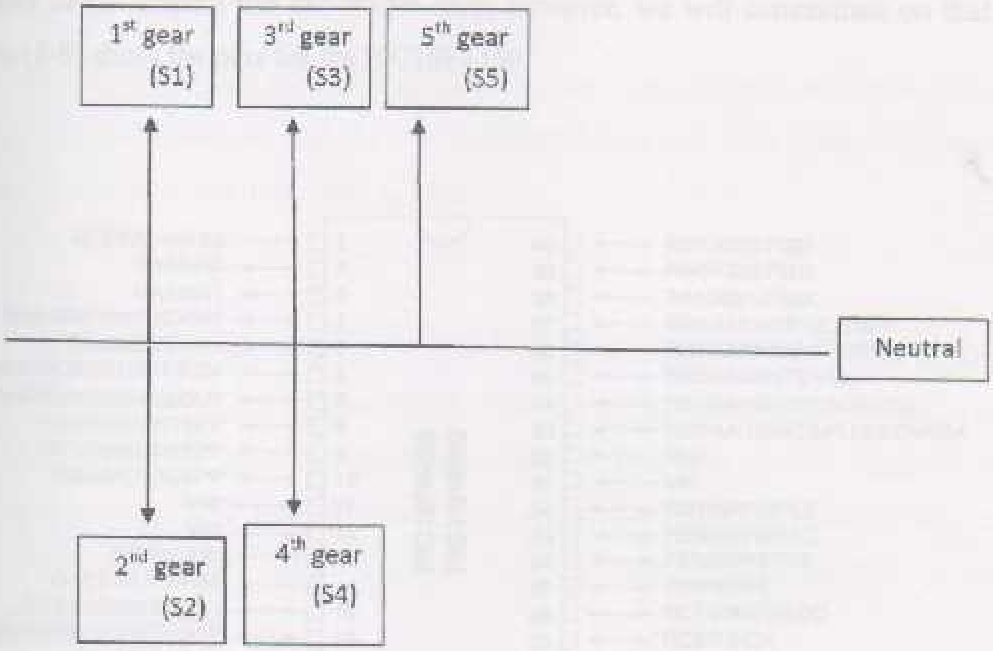

Figure (2-8) gear position sensor

2.2.2.3 The PIC18F4550

The PIC18F4550 family member come in different packages, such as DIP (dual in line package), QFP(quad flat package), and LLC (leadless chip carrier). They all have many pins that are dedicated to various functions such as I/O, ADC, timer, and interrupts. Note that Microchip provides an 18-pin version of the PIC18 family with a reduced number of I/O ports for less demanding applications. Because the vast majority of developers use the 40-pin chip, however, we will concentrate on that. Figure (2-9) shoes the pins for the PIC18F4550.

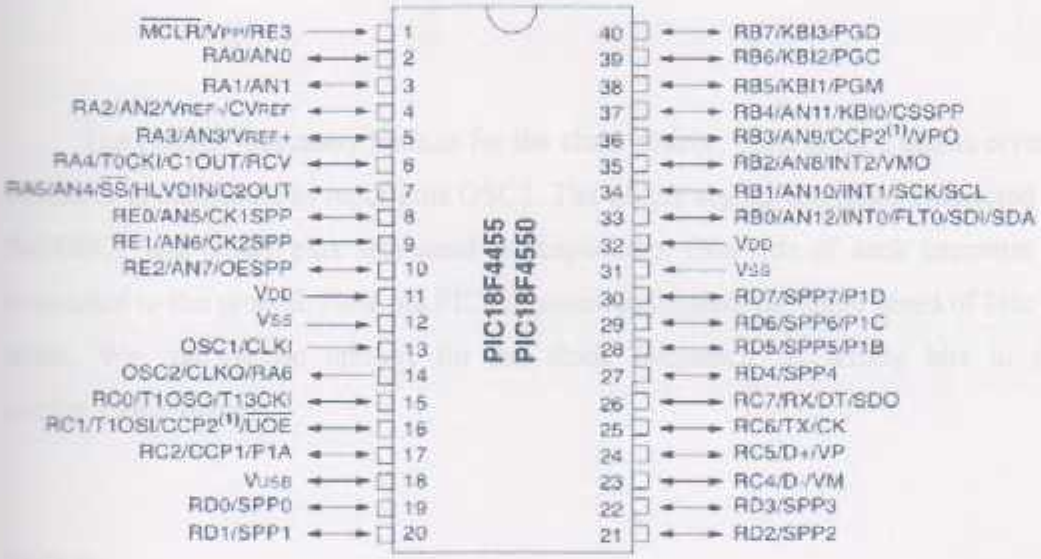

Figure (2-9) microcontroller

Examining Figure (2-9), note that of the 40 pins, a total; of 33 are set aside for the five ports A, B, C, D, and E ,with their alternate functions. The rest of the pin are designated as Vdd, GND (Vss), OSCI, OSC2, and MCLR (master clear reset). Next, we describe the function of each pin. Vdd (Vcc)

Two pins are used to provide supply voltage to the chip. The typical voltage source is +5V. Some PIC18F family members have lower voltage for Vdd pins in order to reduce the noise and power dissipation of the PIC system. We can choose other options for the Vdd voltage level by setting the bits in the configuration register.

Vss(GND):

Two pins are also used for ground, IN chip with 40 pins and more, it is common to have multiple pins for Vcc and GND. This will help reduce the noise (ground bounce) in high-frequency systems.

The PIC18F has many options for the clock source. Most often a quartz crystal oscillator is connected to input pins OSC2. The quartz crystal oscillator connected to the OSC1 and OSC2 pins also needs to capacitors. One side of each capacitor is connected to the ground. Note the PIC18F microcontrollers can have speed of 0Hz to 40Hz. We can choose options for the clock frequency by setting bits in the configuration register.

MCLR:

Pin 1 (in PIC18F4550 40-pin DIP) is the MCLR (master clear reset) pin. It is an input and is active-LOW (normally HIGH). When a LOW pulse is applied to this pin, the microcontroller will reset and terminate all activities.

Port A,B,C,D and E:

The ports PORT A, PORT B, PORT C, PORT D and PORT E, use a total of 33pins. All the ports upon REST are configured as input, because TRIS A –TRISE have the value FFH on them.

PORT A:

Port A occupies a total of 7 pins (RA0-RA6), but for the PIC18F4550, pin A6 is used for OSC2 pin. A6 is not available if we use a crystal oscillator to provide frequency to the PIC18F chip, to use the pins of port A as both input and output ports, each bit must be connected externally to the pin by enabling the bits of the TRISA register.

PORT B:

Port B occupies a total of 8 pins (RB0-RB7). To use the pins of port B as both input and output ports, each bit must be connected externally to the pin by enabling the bits of the register TRISB.

PORT C:

Port C occupies a total of 8 pins (RC0-RC7). To use the pins of port C as both input and output ports, each bit must be connected externally to the pin by enabling the bits of the register TRISC.

PORT D:

Port D occupies a total of 8 pins (RD0-RD7). To use the pins of port D as both input and output ports, each bit must be connected externally to the pin by enabling the bits of the register TRISD.

PORT E:

Port E occupies a total of 3 pins (RE0-RE2) in PIC18F4550. Port E is used for 3 additional analog input or simple I/O: AN5, AN6 and AN7. Just like other ports, port E has alternate functions. [5]

PIC flow chart

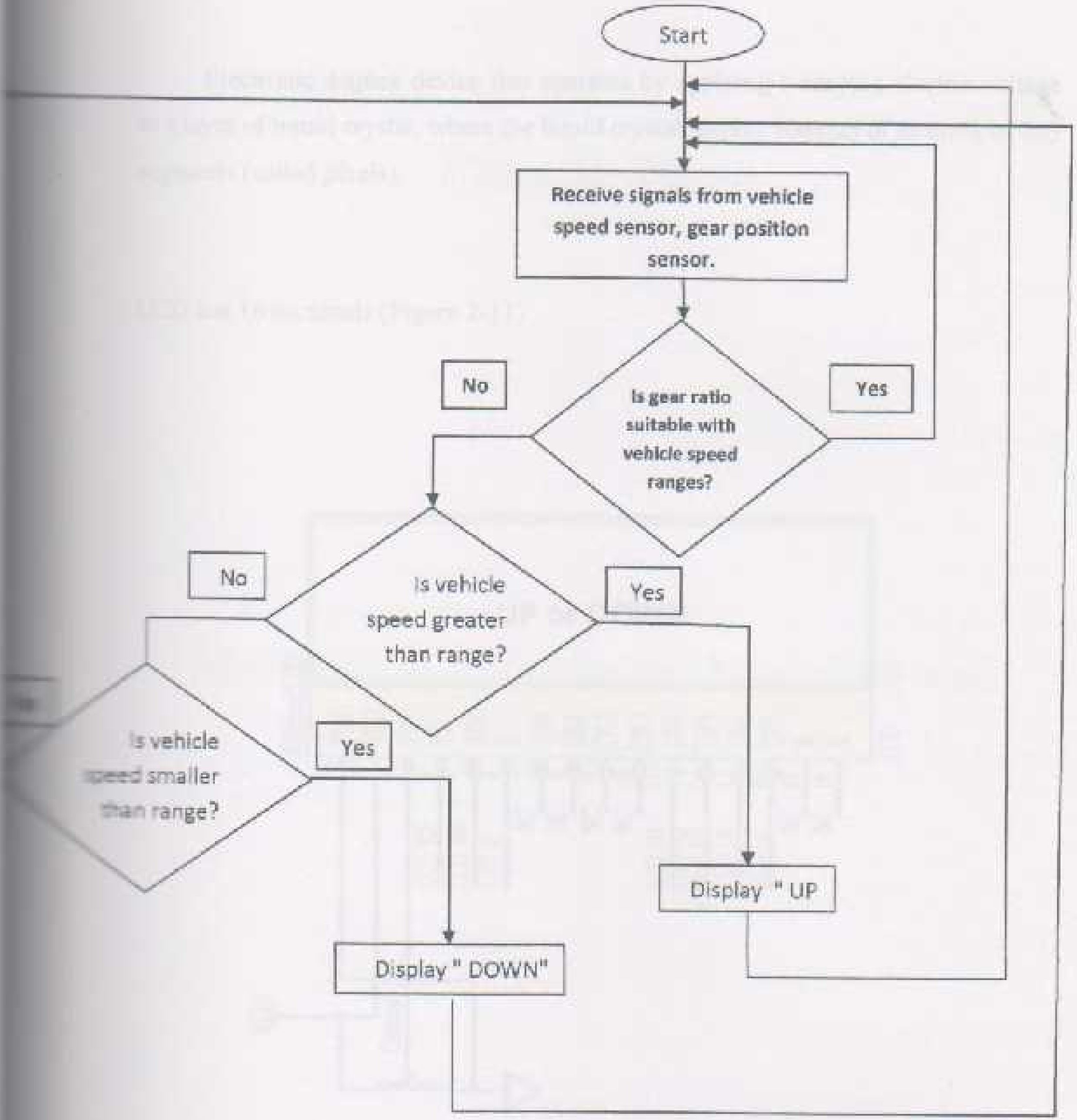

Figure (2-10) Assistance mechanism for choosing suitable gear ratio flow chart

2.2.2.4 Liquid crystal display (LCD)

Electronic display device that operates by applying a varying electric voltage to a layer of liquid crystal, where the liquid crystal display consists of an array of tiny segments (called pixels).

LCD has 16 terminals (Figure 2-11)

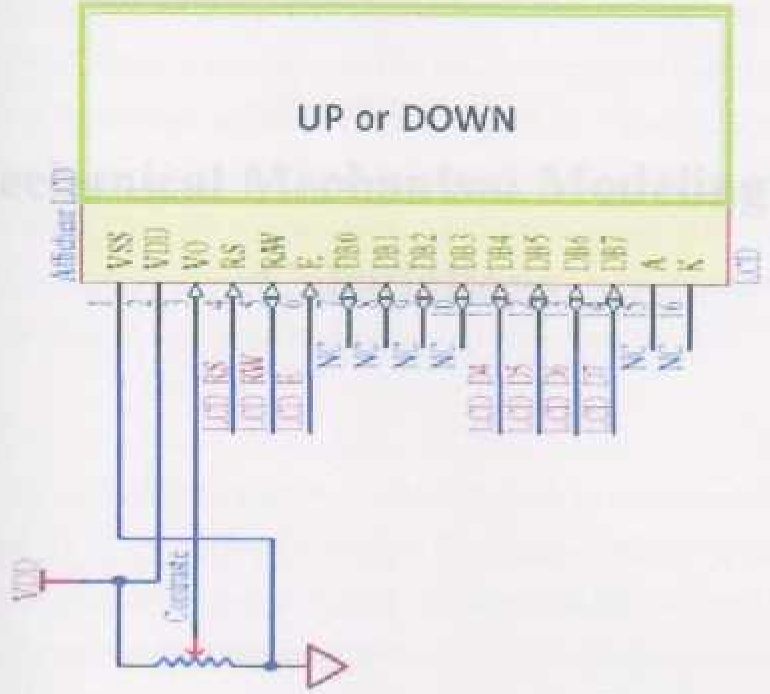

Figure (2-11) LCD terminals

Chapter Three

Mechanical Mechanism Modeling and Calculations

3.1 Introduction

In the field of ergonomics, a growing area of interest is that of the comfort associated with human movement in and around vehicles. There have been few studies to date which have evaluated the comfort associated with human motion when using vehicle commands such as the steering wheel, gear shift and pedals. A pedal transducer was designed and manufactured, and the static and dynamic characteristics of clutch disengagement, engagement were measured for 2 automobiles and a test jury of 13 people. The comfort associated with clutch disengagement, engagement was evaluated by means of a three part questionnaire. Force data measured normal to the pedal surface and postural body angles were correlated against the responses to the questions of the comfort questionnaire. Three parameters were found to strongly correlate with the subjective responses; these were the change of trunk-thigh angle $\Delta\alpha$ from the beginning of the clutch pedal stroke to the end, the maximum force achieved during the end of travel impact, and the average slope of the force – displacement curve during the initial disengagement phase. These quantities appear important in determining clutch actuation comfort and need to be monitored by any device acting as a "clutch meter".

Having achieved important results in areas such as postural comfort [6,16,21] and strength [3,10,7], vehicle ergonomists have begun dedicating effort in recent years towards the study of human motion in and around the vehicle [4,14-15,17,20]. More knowledge regarding human movement strategies [12] and movement comfort [18] would be most beneficial towards the definition of improved design guidelines for vehicles.

This project presents an analysis of automobile clutch pedal actuation. The project addresses the relationship between the subjectively perceived comfort and the mechanical and postural quantities which define the clutch disengagement, engagement process as summarized in (figure3-1).

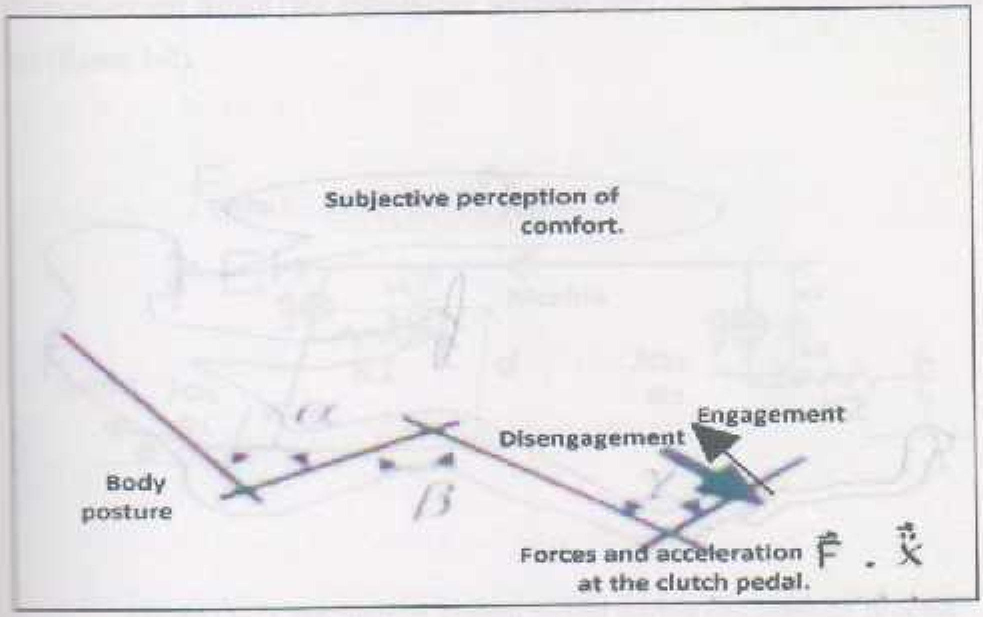

Figure (3-1) The clutch actuation (disengagement, engagement)

Force and acceleration data were measured at the clutch pedal and subjective responses were collected from the test subjects. This permitted a statistical correlation analysis across all pairings of mechanical data versus subjective data, and between all pairings of postural data and subjective response. This project presents the results of the force and postural angle analysis. The results of the analysis of the pedal acceleration data will be the subject of a separate, future project. The analysis described in the following sections represents a first step towards defining design guidelines and perhaps a "clutch meter" device.

3.2 Mathematical mechanical system model

The mathematical mechanical system model during engagement process in disengagement stroke (**for simulation purpose only**) can be represented as shown in the (figure 3-2).

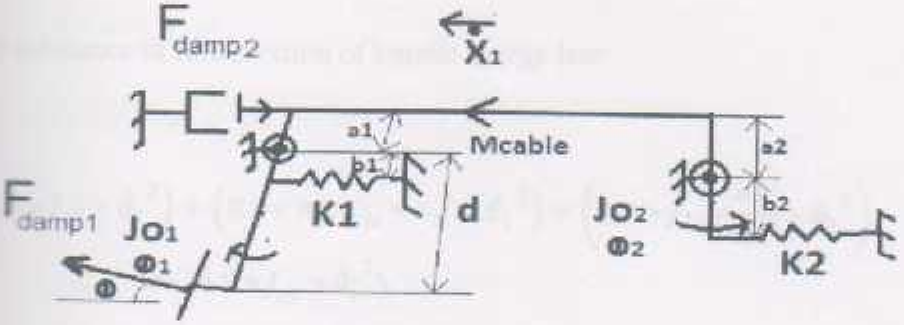

Figure (3-2) Mechanical system model during engagement process

At figure (3-2):

For spring (K1):

$$x_1 = b_1 * \theta_1 = \frac{b_1}{a_1} * x_1$$

For spring (K2):

$$x_2 = b_2 * \theta_2 = \frac{b_2}{a_2} * x_1$$

For damper (C):

$$x_1 = a_1 * \theta_1$$

By applying conservation of kinetic energy law:

$$\sum KE = KE_{eq}$$

$$\left(0.5 * J_{o1} * \dot{\theta}_1^{\,2}\right) + \left(0.5 * m_{cable} * \dot{x}_1^{\,2}\right) + \left(0.5 * J_{o2} * \dot{\theta}_2^{\,2}\right) = \left(0.5 * J_{eq} * \dot{\theta}_1^{\,2}\right)$$

But $x_1 = a_1 * \theta_1$ and $\theta_2 = \frac{a1}{a2} * \theta_1$

By substance in conservation of kinetic energy law:

$$\left(0.5 * J_{o1} * \dot{\theta}_1^{\,2}\right) + \left(0.5 * m_{cable} * a_1^{\,2} * \dot{\theta}_1^{\,2}\right) + \left(0.5 * J_{o2} * \frac{a1^2}{a2^2} * \dot{\theta}_1^{\,2}\right)$$
$$= \left(0.5 * J_{eq} * \dot{\theta}_1^{\,2}\right)$$

$$0.5 * ((J_{o1} + (m_{cable} * a_1^{\,2}) + (J_{o2} * \tfrac{a1^2}{a2^2}))* \dot{\theta}_1^{\,2} = 0.5 * J_{eq} * \dot{\theta}_1^{\,2}$$

$$J_{eq} = (J_{o1} + (m_{cable} * a_1^{\,2}) + (J_{o2} * \tfrac{a1^2}{a2^2}).$$

By applying conservation of potential energy law in springs:

$$\sum U = U_{eq}$$

$$\left(0.5 * K_1 * (b_1 * \theta_1)^2\right) + \left(0.5 * K_2 * (b_2 * \theta_2)^2\right) = \left(0.5 * K_{eq} * \theta_1^{\,2}\right)$$

$$0.5 * \left(\left(K_1 * b_1^{\,2}\right) + \left(K_2 * b_2^{\,2} * \frac{a1^2}{a2^2}\right)\right) * \theta_1^{\,2} = 0.5 * K_{eq} * \theta_1^{\,2}$$

$$K_{eq} = \left(K_1 * b_1^{\,2}\right) + \left(K_2 * b_2^{\,2} * \frac{a1^2}{a2^2}\right).$$

By applying conservation of energy loss law in damper:

$$\sum U_{loss} = U_{eq}$$

$$\left(0.5 * C * (a_1 * \dot{\theta}_1)^2\right) = (0.5 * C_{eq} * \dot{\theta}_1^{\,2})$$

$$\left(0.5 * (C * a_1^{\,2}) * \dot{\theta}_1^{\,2}\right) = (0.5 * C_{eq} * \dot{\theta}_1^{\,2})$$

$$C_{eq} = \boldsymbol{C} * \mathbf{a}_1^{\,2}.$$

By applying Newton second law about O_1:

$$J_{eq} * \ddot{\theta}_1 + C_{eq} * \dot{\theta}_1 + K_{eq} * \theta_1 = -(F_{damp2} * \cos(\theta) * d)$$

$$\ddot{\theta}_1 + \frac{C_{eq} * \dot{\theta}_1}{J_{eq}} + \frac{K * \theta_1}{J_{eq}} = \frac{-(F_{damp2} * \cos(\theta) * d)}{J_{eq}}$$

$$\omega_n = \sqrt{\frac{K_{eq}}{J_{eq}}}$$

$$2 * \xi * \omega_n = \frac{C_{eq}}{J_{eq}} \rightarrow \xi = \frac{C_{eq}}{J_{eq} * 2 * \omega_n}$$

but $C_{eq} = \boldsymbol{C} * \mathbf{a}_1^{\,2}$ *and* $C = f(D, d, \rho)$.

Where:

D: Diameter of pneumatic chock absorber cylinder.

d: Diameter of exhaust , inlet port.

ρ: *fluid density*.

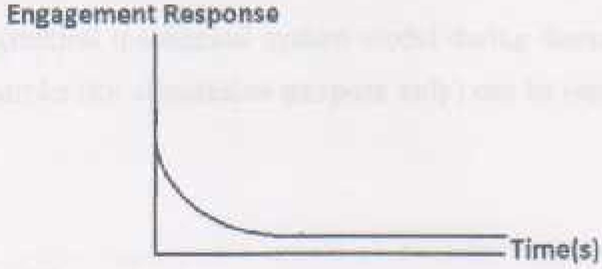

Figure (3-3) Engagement process response

$\xi = 1$ (critically damped response) (figure 3.3) which means:

→ the response without overshoot .

→ exponantioal response(smooth response).

3.3 Mathematical mechanical system model

The mathematical mechanical system model during disengagement process in disengagement stroke (for **simulation purpose only**) can be represented as shown in the (figure 3-4).

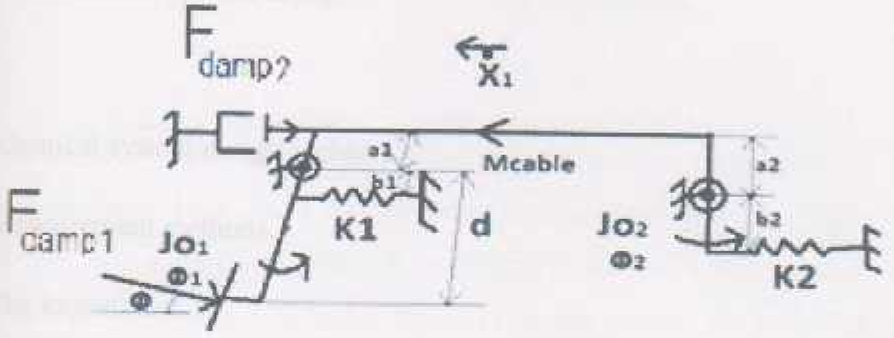

Figure (3-4) Mechanical system model during disengagement process

$$J_{eq} = (J_{o1} + (m_{cable} * a_1^{\,2}) + (J_{o2} * \frac{a1^2}{a2^2}).$$

$$K_{eq} = (K_1 * b_1^{\,2}) + \left(K_2 * b_2^{\,2} * \frac{a1^2}{a2^2}\right).$$

$$C_{eq} = C * a_1^{\,2}.$$

$$J_{eq} * \ddot{\theta}_1 + C_{eq} * \dot{\theta}_1 + K_{eq} * \theta_1 = (F_{damp2} * \cos(\theta) * d)$$

$$\ddot{\theta}_1 + \frac{C_{eq} * \dot{\theta}_1}{J_{eq}} + \frac{K * \theta_1}{J_{eq}} = \frac{(F_{damp2} * \cos(\theta) * d)}{J_{eq}}$$

$$\omega_n = \sqrt{\frac{K_{eq}}{J_{eq}}}$$

$$2 * \xi * \omega_n = \frac{C_{eq}}{J_{eq}} \rightarrow \xi = \frac{C_{eq}}{J_{eq} * 2 * \omega_n}$$

3.4 Mechanical system design

Mechanical system design includes:

1. Measurement methods.

2. The experiment.

3. Results of clutch (disengagement, engagement) forces, questionnaire responses, correlation analysis.

4. Sizing pneumatic chock absorber.

1. Measurement methods

This project measured the normal forces at the clutch pedal both statically and dynamically. A static test of each automobile's clutch pedal was performed using a spring loaded force gauge (Salter Model 16 Tension and Compression Tester) which was pushed against the pedal surface to measure the force. A gravity goniometer was attached at a convenient point along the pedal body to measure the angle φ from which the pedal rotation angle θ could be calculated (figure 3-5).

Figure (3-5) Clutch pedal sensor

The force gage was pressed against the centre of the clutch pedal at 90 degrees to the surface. Five force measurements were attempted at roughly 2 degree intervals, but it was not possible to complete all the measurements due to the difficulty of manually stabilizing the force gauge against the pedal while working inside the automobile. Those angles for which it was possible to obtain three measurements were averaged together to obtain the static force-deflection curve.

Dynamic measurements were made by means of a sensor designed for this project which is shown in (figure 3-6) mounted on the clutch pedal of a Ford Fiesta.

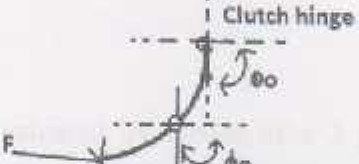

Figure (3-6) Static measurements of clutch force

The sensor consisted of two steel attachment plates which were tightened together to trap the automobile clutch pedal, thus fixing the sensor to the pedal. A third steel plate was separated from the other two by two B&K type 8200 piezoelectric force sensors. One force sensor was located on each side of the pedal centerline, thus the total normal force acting on the pedal sensor was calculated during post processing as:

$$F_{total} = F_{left} + F_{right}$$

A PCB model 336C04 piezoelectric accelerometer was attached to the back surface of the pedal sensor to measure the linear acceleration during actuation. The whole pedal sensor unit weighed 250 grams. The charge signal from each force sensor was amplified by means of B&K type 2635 amplifiers while the PCB accelerometer furnished a voltage signal directly due to the sensor's ICP amplifier and the use of a PCB model 480D09 power supply. The force and acceleration signals were recorded by means of an 8 channel KYOWA RTP-610 analogue tape recorder. Signal analysis was performed in the laboratory using the Time Data Processing Monitor (TMON) of the LMS CADA-X revision 3.4 software system [11]. The LMS software was run on an HP 715/64 workstation with a Difa Measuring Systems SCADAS II front end unit. After a series of preliminary evaluations, it was found that a sampling rate of 1000HZ (500 HZ cut-off) was necessary to obtain precise values for the peak force during end of travel impact.

Subjective comfort was evaluated by means of a 3 part questionnaire. The questionnaire was developed by performing tests with 3 people prior to the project described in this project. The questionnaire sections were:

1. A general comfort evaluation form.

2. A body part discomfort form.

3. A pedal mechanical evaluation form.

A general comfort evaluation form.

Most questions were presented using a tow step Likert type format. A two-step scale was used to extend the optimum number of response options beyond the 5 to 7 range typical of one step Likert scales [5, 13]. Question number 3 of the general comfort evaluation form is given as an example in (figure 3-7).

How do you rate the general level of comfort when actuating the clutch pedal?

Very Uncomfortable		Uncomfortable		average		Comfortable		Very comfortable	
1	2	3	4	5	6	7	8	9	10

Figure (3-7) a question from the general comfort section of the questionnaire

A body part discomfort form.

The body part discomfort from asked the test subjects to state the level of comfort associated with each of the 11 body regions identified in (figure 3-8). Each region had an associated 10 point scale like the one of (figure 3-7). Eleven regions were used so as to localize the body sensations precisely, with specific muscle packs being targeted in the case of the leg segments.

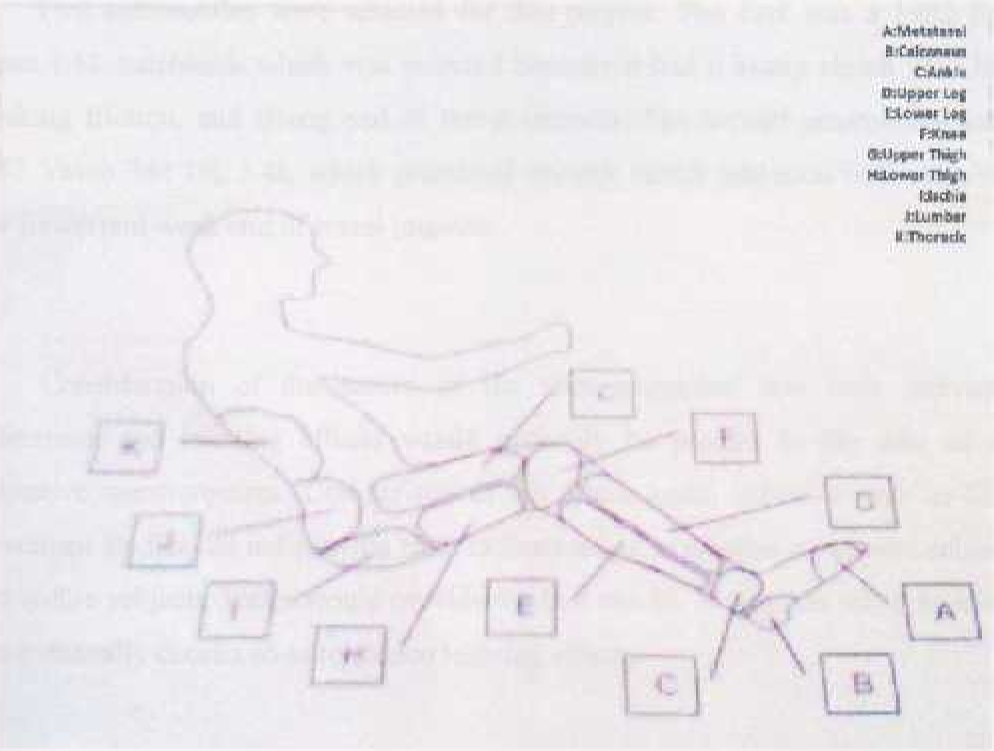

Figure (3-8) Body regions evaluated in the body part discomfort form

Three body angles were measured and analyzed in this project to define the seated posture of the test subject. The angles were α, β and γ which are defined in (figure 3.1) and which were measured by means of a full circle goniometer with 12 inch arms. Each angle was measured for each subject in two test positions, the beginning and the end of the clutch pedal stroke.

2. The experiment

Two automobiles were selected for this project. The first was a 1982 Ford Fiesta 1.1L hatchback which was selected because it had a heavy clutch with high breaking friction, and strong end of travel impacts. The second automobile was a 1987 Volvo 340 DL 1.4L which presented smooth clutch actuation with relatively low forces and weak end of travel impacts.

Consideration of the nature of the tests suggested that both individual differences and learning effects would probably be present in the data of the subjective questionnaires. Comparison of the clutch pedal actuation task to other movement studies did not provide clear indications as to whether a between subjects or a within subjects design would provide the best results. A between subjects design was eventually chosen so as to reduce learning effects.

Thirteen subjects took part in the experiment. Six (4 male and 2 female) tested the Fiesta while seven (4 male and 3 female) tested the Volvo. The subjects were all students, with a mean age of 22.9 and a range from 21 to 26 years. None suffered from any physical disability and none were informed of the nature of the study until the day of the test. Nationality was diverse; the subjects came from 6 nations. The subjects were asked to wear light clothing and most arrived for the tests dressed in trousers and light shirts. Twelve of the subjects wore light and flexible trainers or town shoes, while one wore heavy boots. Each subject performed one test with one of the two automobiles. The automobile was stationary in an open parking lot with the motor off. Each test took roughly 30 minutes to perform and consisted of the following phases:

Table 3.1 Phases of the test procedure

Phase	Tasks performed and information obtained.
Participation form(3 minutes)	The subject was asked to read the instructions describing the intended purpose and nature of the experiments and to sign a consent agreement to participate.
Driving posture adjustment (4 minutes).	The subject was asked to adjust the seat and other systems and to attach the belts. The subject was then asked to simulate a driving task as realistically as possible , and to readjust all parameters as many times as necessary until a comfortable driving posture was reached which guaranteed good outside visibility.
Subject data form (2 minutes).	The subject was asked to furnish several general information such as age, physical disabilities, sports practiced and interests. The subject was then measured in several anthropometric dimensions.
Measurement of postural angles (4 minutes).	The body angles α ,β and γ were measured in tow positions : with the foot just contacting the clutch pedal (start of stroke) and with the pedal completely depressed (end of stroke).

Clutch usage task (8 minutes).	The subject was instructed to perform 8 minutes of pedal actuation at a fast fixed rhythm so as to induce some muscle fatigue . he subject was instructed to analyze the situation as carefully as possible.
Subjective questionnaire (6-8 minutes).	The subject was asked to fill out the 3 part questionnaire (total of 4 pages) as carefully as possible
Actuation recording (1-2) minutes.	The subject was asked to run through the gears in the sequence 1-2-3-4-3-2-1. It was asked that gear changes be vigorous as preliminary tests had shown that the force sensors were not accurate for very slow (low frequency) movements.

3. Results of clutch disengagement forces, questionnaire responses, correlation analysis.

Results of clutch disengagement forces.

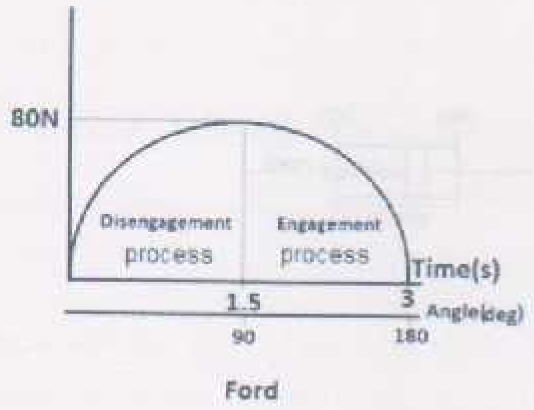

Figure 3-9 below presents the results from the static tests of the two cars (**for design purpose**).

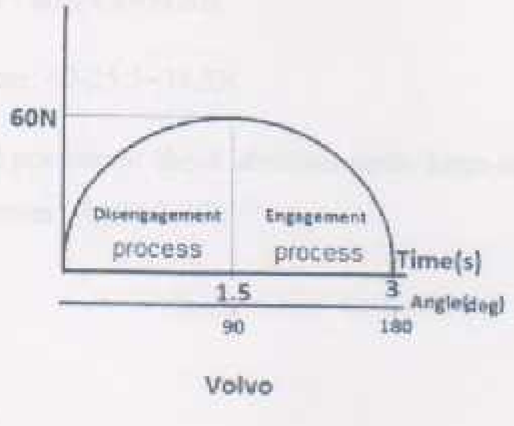

Figure (3-9) Static force-angle/time curves for ford and the Volvo

Reduction maximum static force

Assume Ford and Volvo has same pedal travel=0.12m , pneumatic chock absorber cylinder diameter=0.018m , air density=1.22Kg/M^3 , Patm=10^{5}pa.

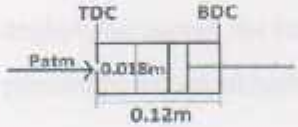

$$F_{damp} = (P_{atm} * A_{piston}) + (\rho_{air} * g * pedal\ travel * A_{piston})$$

$$\left(10^5 * \frac{\pi * 0.018^2}{4}\right) + (1.22 * 9.81 * 0.12 * \frac{\pi * 0.018^2}{4}) \rightarrow 25.5N$$

For ford car : 80-25.5=54.5N.

For Volvo car: 60-25.5=34.5N.

After added pneumatic chock absorber static force-angle/time curves for ford and the Volvo becomes (figure 3-10):

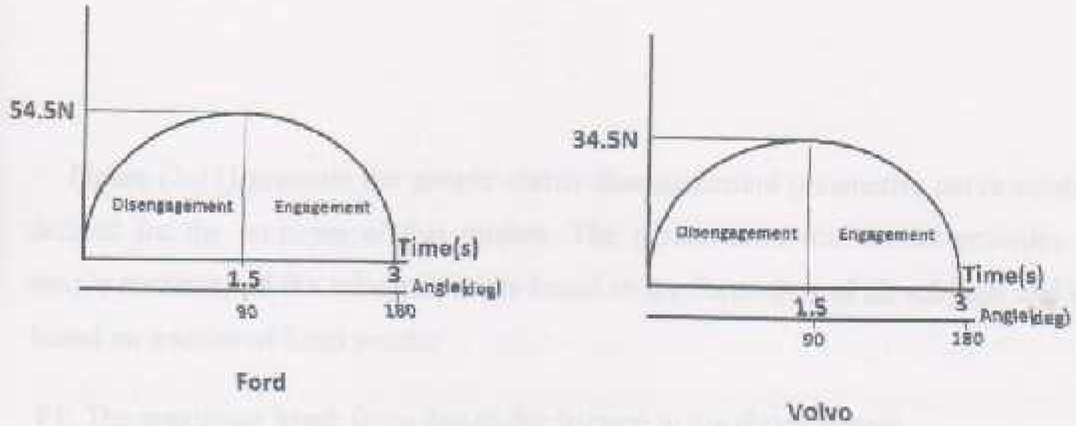

Figure (3-10) Static force-angle/time curves for ford and the Volvo after added pneumatic chock absorber

It can be seen that the Ford presented higher disengagement forces and used a smaller angular range than did the Volvo. While the differences in angular range were probably due to design, the force differences could simply reflect differences in clutch wear [9]. The static curves were measured in equilibrium, therefore they do not show the force build up due to dry friction in the clutch system or the force at the end of the disengagement stroke due to the end of travel impact.

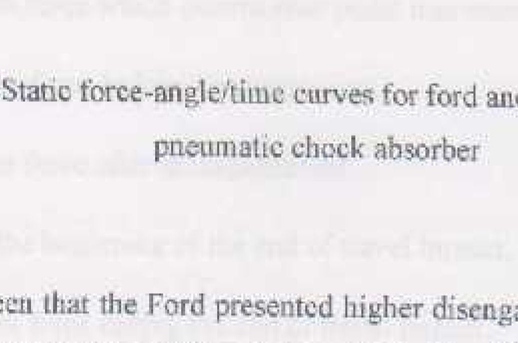

Figure (3-11) Clutch disengagement parametric curve model

Figure (3-11) presents the *simple* clutch disengagement parametric curve model defined for the purposes of this project. The parametric curve model provides a simple summary of the salient features found in the force data of all subjects and is based on a series of fixed points:

F1: The maximum break force due to dry friction in the clutch system.

F2: The minimum force which occurs after pedal movement begins.

F3: The maximum force before disengagement.

F4: The minimum force after disengagement.

F5: The force at the beginning of the end of travel impact.

F6: The maximum force during the end of travel impact.

The values at all 6 points were read from the force time histories of all five tests of each subject. Besides the force values themselves, the time intervals between points and the average slopes from point to point were also recorded.

The force rise due to dry friction was found to be as high as 10N in the case of the Ford, while the Volvo presented little evidence of dry friction. The end of travel impact was found to produce high forces in both cars. The mean value found across all tests of the two cars was 124N with a standard deviation of 38N. The maximum value recorded was 200N. On average, the end of travel impact represented a 32% increase over the maximum force before disengagement (point3).

The repeatability of the force time histories was found to be high for each subject if they were keeping to a fixed rhythm. Of the six forces of clutch disengagement parametric curve model, the one which varied most across tests of the same subject (lowest repeatability) was the maximum force during the end of travel impact (point6). The subject with the highest repeatability for the impact produced a mean value of 150N and had a standard deviation of 10N. The subject with the lowest produced a mean force value of 190N and a standard deviation of 30 N.

The force curves were found to be quite different for the Ford Fiesta and the Volvo 340, with the Ford curves being generally higher. For example, the force at the point 3 before disengagement was found to be more that 25% higher on the static curves and an average of 21% higher on the dynamic curves. The Ford also had a very strong force rise due to dry friction which was almost totally absent in the case of the Volvo, and the Ford also had the larger end of travel impact.

Reduction maximum dynamic force

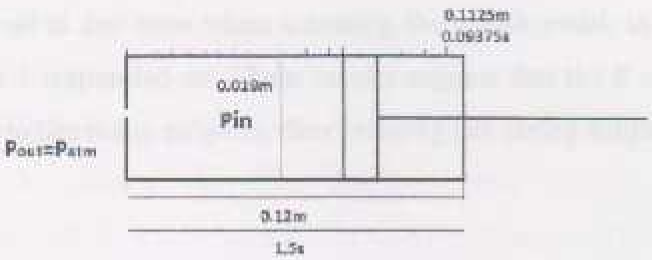

$$F_{damp}(t) = \left(\frac{dp_{in}}{dt} * A_{piston}\right) + (P_{atm} * A_{piston})$$

$$F_{damp}(t)_{max} \ when \frac{dp_{in}}{dt} \ is \ max.$$

$$But \frac{dp_{in}}{dt} = \rho_{air} * g * velocity \rightarrow \frac{dp_{in}}{dt} \ is \max when \ velocity \ is \ max.$$

$$But \ velocity(t) = \frac{stroke}{t}$$

$$velocity_{max} = \frac{0.1125}{0.09375} = 1.2m/s$$

$$F_{damp}(t = 0.09375s)_{max}$$

$$= \left(1.22 * 9.81 * 1.2 * \frac{\pi * 0.018^2}{4}\right) + \left(10^5 * \frac{\pi * 0.018^2}{4}\right) = 25.5N$$

For both cars: 150-25.5=124.5N.

Results: Questionnaire Responses

The first question asked whether feelings of discomfort were experienced at any time when actuating the clutch pedal, 9 subjects responded yes while 4 responded no. The second question asked whether feelings of fatigue were experienced at any time when actuating the clutch pedal, in this case 10 responded yes while 3 responded no. These results suggest that the 8 minute clutch usage task managed to tire many subjects, thus bringing out strong subjective impressions.

The force differences between the two cars at all six disengagement model points were found to be higher than the Weber Fraction determined by Southall [19] for pedal force perception (7%). Therefore the human subjects would in practice be expected to perceive such force differences, and it might be expected that this would translate into differences between the two automobiles in the subjective questionnaire results. T-tests were calculated (11 degree of freedom) for all questions of the subjective questionnaire. Statistically significant differences were found between the results of the two automobiles in the case of three questions:

1. The body part discomfort rating for the lower leg region E ($p<0.01$).

2. The body part discomfort rating for the upper thigh region G ($P<0.05$).

3. The question "How much resistance did you encounter when pushing the clutch?"($P<0.05$).

The Ford was rated more comfortable than the Volvo in the case of the lower leg (region E) while the opposite was true for the upper leg (region G). Interestingly, the Volvo was rated as having the highest pedal resistance even through the force curves was generally lower.

The final three questions asked whether the presence of the pedal transducer interfered with the subject's natural movement and comfort. A 10 point scale similar to that of figure 3.9 was used with "not at all" being assigned a value of 1 and "very strongly" a value of 10. The average values and standard deviations were 2.54(sigma=1.27), 1.85(sigma=1.14) and 2.23(sigma=1.36) suggesting that the presence of the transducer should have had only a minimal effect on clutch actuation task.

Results: Correlation Analysis

A general correlation analysis was performed by calculating Pearson r coefficients [5,8] between all possible pairings of mechanical versus subjective values, and between all possible pairing of postural versus subject values. The objective was to identify the quantities which most affected human perception of comfort during clutch disengagement. Force values, slope values, time values, postural angle values and questionnaire results were assembled and correlated.

Since 13 subjects were used and 2 variables were correlated each time, the number of statistical degrees of freedom was 11. For 11 degrees of freedom any r value in excess of r=0.553 is to be considered significant at a 95 percent confidence level [8]. Nine data pairings produced a Pearson r coefficient higher than r=0.553. The mechanical and postural parameters involved were:

1. The change in the thigh – trunk angle $\Delta\alpha=\alpha2-\alpha1$.

2. The maximum end of travel impact force at point 6.

3. The slope from point 5 to 6 during end of travel impact.

4. The slope between points 2 and 3 before disengagement.

Figure (3-9) presents the data, the fitted regression lines, and the portion of the variance accounted for (r^2) for the nine data pairs. The highest Pearson r coefficients were found between the change in trunk- thigh angle ($\Delta\alpha=\alpha2-\alpha1$) and four of the general subjective responses. $\Delta\alpha$ accounted for more than 60 percent of the variance for two of the questionnaire responses. For all questionnaire responses the level of comfort increased as $\Delta\alpha$ increased. Significant correlations were also found for the end of travel impact force, the end of travel impact slope and the slope of the force curve before disengagement(from point2 to 3). While these correlations were weaker, the size of the effect was actually greater in several cases such as the end of travel impact force and slope. It was interesting to find that comfort actually rose with rising force or slope in several cases.

4. Sizing pneumatic chock absorber.

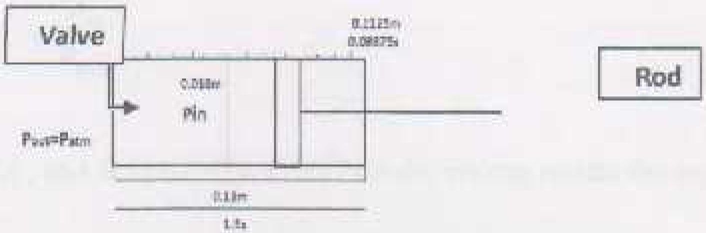

Capacity coefficient or flow factor:

$$C_V = \frac{Q}{22.48} * \sqrt{\frac{G * T}{(P_{in} - P_{out}) . P_{out}}} \rightarrow$$

$$Q = C_V * 22.48 * \sqrt{\frac{G * T}{(P_{in} - P_{out}) . P_{out}}} \left(\frac{ft^3}{minute}\right).$$

To simplify the equation, experts typically assume a conservative pressure change between in and out ($P_{in} - P_{out}$) of 5 psi.

For time or process-critical applications, reduce this to 2 psi. And, in many cases, a pressure drop of 10 psi is not detrimental to the application. A 10-psi pressure drop permits smaller valves that lower costs and require less mounting space.

To simplify calculations, let's tabulate values for a portion of the equation for 2, 5, and 10-psi pressure changes. Here, we create a constant A, defined as:

$$A = \frac{1}{22.48} * \sqrt{\frac{G * T}{(P_{in} - P_{out}) * P_{out}}}$$

This reduces the flow-coefficient equation to $C_v = QA$. In terms of cylinder volume and time:

$$Q = \frac{Volume * P_{in}}{28.8 * t * P_{out}}$$

Restating the volumetric flow rate equation in terms of compression ratio results in:

$$Q = \frac{V * C_r}{28.8 * t} \text{ where } C_r = \frac{P_{in}}{P_{out}}$$

Given that $C_v = Q*A$, and *Volume* = $(\pi/4)*D^2*stroke$, we can restate the equation as:

$$C_V = \left(\frac{\left(\frac{\pi}{4}\right) * C_r * A}{28.8}\right) * \left(\frac{stroke}{t}\right) * (D^2).$$

Here, stroke/t is a simplified representation of average rod velocity in inches per second.

But because designers usually specify ISO cylinders in metric units, apply the conversion factor 1 in = 25.4 mm and revise the equation:

$$C_V = \left(\frac{\left(\frac{\pi}{4}\right) * C_r * A}{28.8 * 25.4^3}\right) * \left(\frac{stroke}{t}\right) * (D^2).$$

Nomenclature:

D = Pneumatic chock absorber cylinder diameter (m).

G = Specific gravity of the fluid (G = 1 for air).

Q = Volumetric flow rate (m^3/s).

T = Absolute temperature of air (K).

t = Time to fill cylinder (sec).

Table 3.2 *Cv* VALUES FOR TWO-POSITION VALVES

C_v VALUES FOR TWO-POSITION VALVES

Cv Values - Highlighted for 2-Position ISO Valves

Average Rod Speed (mm/s)	Cylinder Diam (mm)														
	8	10	12	16	20	25	32	40	50	63	80	100	125	160	200
25	0.001	0.001	0.002	0.003	0.005	0.008	0.013	0.021	0.032	0.051	0.083	0.129	0.202	0.331	0.517
50	0.002	0.003	0.004	0.007	0.010	0.016	0.026	0.041	0.065	0.103	0.166	0.259	0.404	0.662	1.035
75	0.002	0.004	0.006	0.010	0.016	0.024	0.040	0.062	0.097	0.154	0.248	0.388	0.606	0.994	1.552
100	0.003	0.005	0.007	0.013	0.021	0.032	0.053	0.083	0.129	0.205	0.331	0.517	0.809	1.325	2.070
125	0.004	0.006	0.009	0.017	0.026	0.040	0.066	0.103	0.162	0.257	0.414	0.647	1.011	1.656	2.587
150	0.005	0.008	0.011	0.020	0.031	0.049	0.079	0.124	0.194	0.308	0.497	0.776	1.213	1.987	3.105
175	0.006	0.009	0.013	0.023	0.036	0.057	0.093	0.145	0.226	0.359	0.580	0.906	1.415	2.318	3.622
200	0.007	0.010	0.015	0.026	0.041	0.065	0.106	0.166	0.259	0.411	0.662	1.035	1.617	2.649	4.140
225	0.007	0.012	0.017	0.030	0.047	0.073	0.119	0.186	0.291	0.462	0.745	1.164	1.819	2.981	4.657
250	0.008	0.013	0.019	0.033	0.052	0.081	0.132	0.207	0.323	0.513	0.828	1.294	2.021	3.312	5.174
275	0.009	0.014	0.020	0.036	0.057	0.089	0.146	0.228	0.356	0.565	0.911	1.423	2.223	3.643	5.692
300	0.010	0.016	0.022	0.040	0.062	0.097	0.159	0.248	0.388	0.616	0.994	1.552	2.426	3.974	6.209
325	0.011	0.017	0.024	0.043	0.067	0.105	0.172	0.269	0.420	0.667	1.076	1.682	2.628	4.305	6.727
350	0.012	0.018	0.026	0.046	0.072	0.113	0.185	0.290	0.453	0.719	1.159	1.811	2.830	4.636	7.244
375	0.012	0.019	0.028	0.050	0.078	0.121	0.199	0.310	0.485	0.770	1.242	1.940	3.032	4.968	7.762
400	0.013	0.021	0.030	0.053	0.083	0.129	0.212	0.331	0.517	0.822	1.325	2.070	3.234	5.299	8.279
425	0.014	0.022	0.032	0.056	0.088	0.137	0.225	0.352	0.550	0.873	1.407	2.199	3.436	5.630	8.797
450	0.015	0.023	0.034	0.060	0.093	0.146	0.238	0.373	0.582	0.924	1.490	2.329	3.638	5.961	9.314
475	0.016	0.025	0.035	0.063	0.098	0.154	0.252	0.393	0.614	0.975	1.573	2.458	3.840	6.292	9.832
500	0.017	0.026	0.037	0.066	0.103	0.162	0.265	0.414	0.647	1.027	1.656	2.587	4.043	6.623	10.349

These tables chart flow requirements based on cylinder size and average rod speed. The large table highlights two-position ISO valves that meet the needed C_v, assuming 80 PSI inlet pressure and 5 PSI pressure drop.

In this project: $D_{cylinder} = 18mm$,

$$average\ rod\ speed = \frac{stroke}{t} = \frac{120}{1.5} = \frac{80mm}{s}.$$

From table(3.2): CV=0.016.

From table (3.3):

$when\ C_v = 0.55 \rightarrow valve\ size = 18mm$

$But\ when\ C_v = 0.016 \rightarrow valve\ size = 0.523mm.$

$P_{in_{abs}} = (\rho_{air} * g * stroke) + P_{atm} = (1.22 * 9.81 * 0.12) + 10^5 = 100001.5pa$

$P_{out_{abs}} = 10^5 pa$

$$C_r = \frac{P_{in}}{P_{out}} = \frac{100001.5}{10^5} = 1.1 \rightarrow A = 0.103.$$

$$t = \frac{D^2 * stroke * \left(\frac{\pi}{4}\right) * C_r * A}{C_v * 28.8 * 25.4^3} = \frac{18^2 * 120 * \left(\frac{\pi}{4}\right) * 1.1 * 0.103}{0.016 * 28.8 * 25.4^3} = 0.5s$$

Table 3.3 VALVE RATINGS and BASIC DATA

VALVE RATINGS

ISO Valve Size	FH Designation	C_v Values	
		Two Position	Three Position
18 mm	H8	0.55	[illegible]
26 mm	[illegible]	1.1	1.0
Size 1	H1	[illegible]	1.2
Size 2	H2	3.0	[illegible]
Size 3	H3	[illegible]	[illegible]

These tables chart flow requirements based on cylinder size and average rod speed. The large table highlights two position ISO valves that meet the needed Cv.

BASIC DATA

Inlet Pressure (PSIG)	Compression Factor	A Constants		
		2 PSI ΔP	5 PSI ΔP	15 PSI ΔP
10	1.7	[illegible]	.103	
20	2.4	[illegible]	[illegible]	[illegible]
30	3.0	.111	[illegible]	[illegible]
40	3.7	.100	[illegible]	[illegible]
50	4.4	.091	[illegible]	[illegible]
60	5.1	.085	[illegible]	[illegible]
70	5.8	.079	.051	[illegible]
80	[illegible]	.075	[illegible]	[illegible]
90	7.1	.071	[illegible]	[illegible]
100	7.8	[illegible]	[illegible]	[illegible]
110	[illegible]	[illegible]	[illegible]	[illegible]
120	[illegible]	[illegible]	[illegible]	[illegible]
130	[illegible]	[illegible]	[illegible]	[illegible]
140	10.5	[illegible]	.037	[illegible]
150	11.2	[illegible]	[illegible]	[illegible]
160	[illegible]	[illegible]	[illegible]	[illegible]
170	[illegible]	[illegible]	[illegible]	[illegible]
180	[illegible]	[illegible]	[illegible]	[illegible]
190	[illegible]	[illegible]	[illegible]	[illegible]
200	[illegible]	[illegible]	[illegible]	[illegible]

The table lists compression ratios, P_1/P_a, as well values for the constant A, for a range of inlet pressures and pressure drops.

Chapter Four

Analysis And Control Of An Assistance Mechanism For Choosing Suitable Gear Ratio

4.1 Introduction

Movement of different parts of any device, or even movements of the human body are meaningless and useless without control to serve the purpose and objective of this movement.

This concept from the meaning of control is clear to reach the intended target of the movement. And in order for that the control system must have the main components of control operations; the signal is receiving from input and then processed, and sent to the output to return the signal through the feedback and comparison with the input, so when the feedback signal is equal with the input this means that the target is reached, figure (4-1). And when adding a controller in the system, it makes processing of characteristics including achieve the desired goal quickly and accurately figure (4-2).

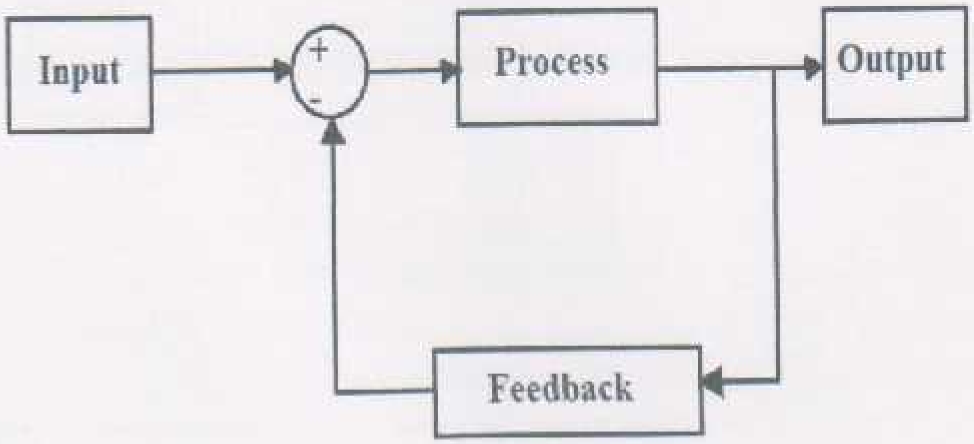

Figure (4-1) Block diagram represents the system without controller

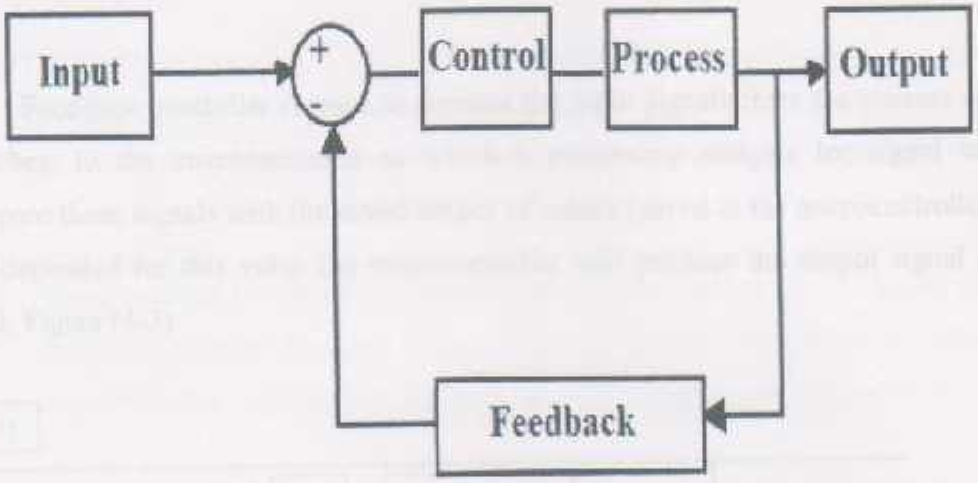

Figure (4-2) Block diagram represents the system with controller

4.2 How to control

Feedback controller is used to connect the input signals from the sensors and switches, to the microcontroller in which a processing analysis for signal will compare these signals with the saved ranges of values (saved in the microcontroller), and depended for this value the microcontroller will produce the output signal on LCD, Figure (4-3).

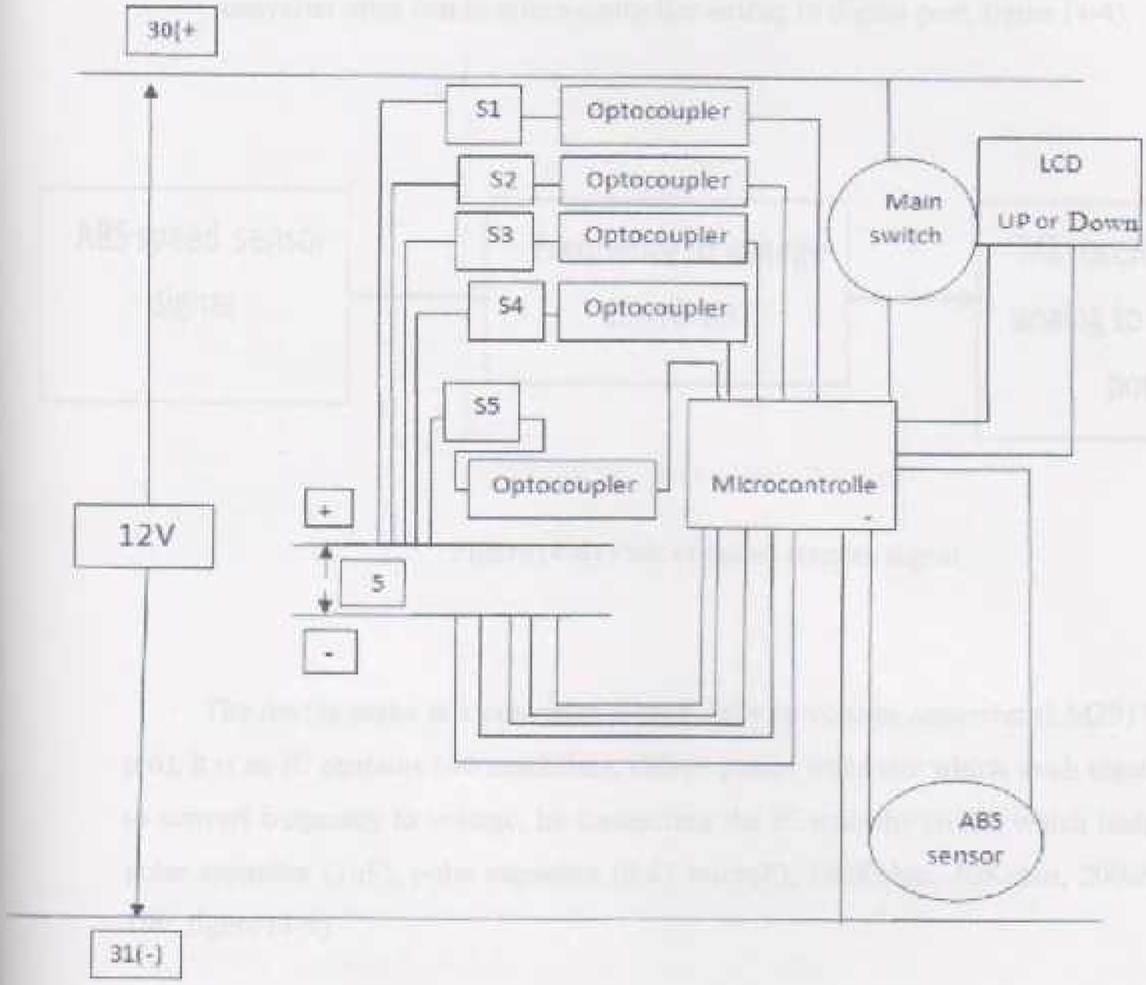

Figure (4-3) Block diagram represents inputs and outputs of the microcontroller

4.3 Sensors

Sensors collect information and convert it to the controller; two types of sensors have been used in the proposal system; speed sensors and gear position sensor:

1. Speed sensors (frequency generator): this sensor creates an AC signal with frequency relative to speed. Then, these signals enter frequency to voltage converter after that to micro controller analog to digital port, figure (4-4).

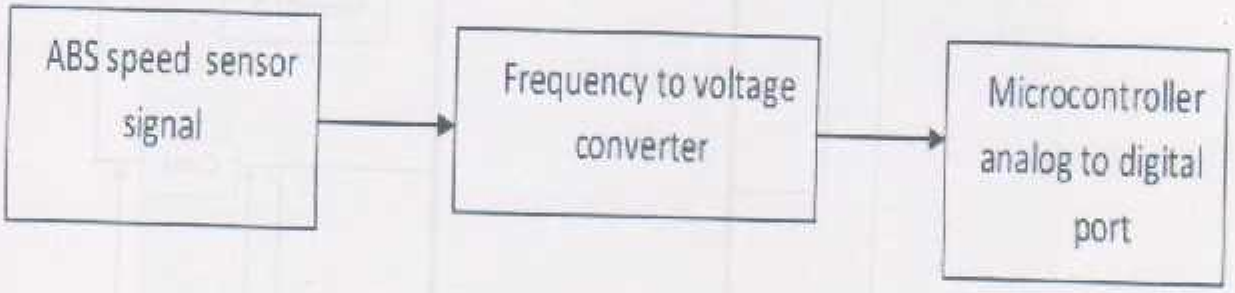

Figure (4-4) Path of speed sensors signal

The device make this converter is frequency to voltage converter (LM2917 8-pin), it is an IC contains two amplifiers, charge pump, transistor which work together to convert frequency to voltage, by connecting the IC with the circuit which include polar capacitor (1nF), polar capacitor (0.47 microF), 100Kohm, 10Kohm, 200ohm, 10v, figure (4-5).

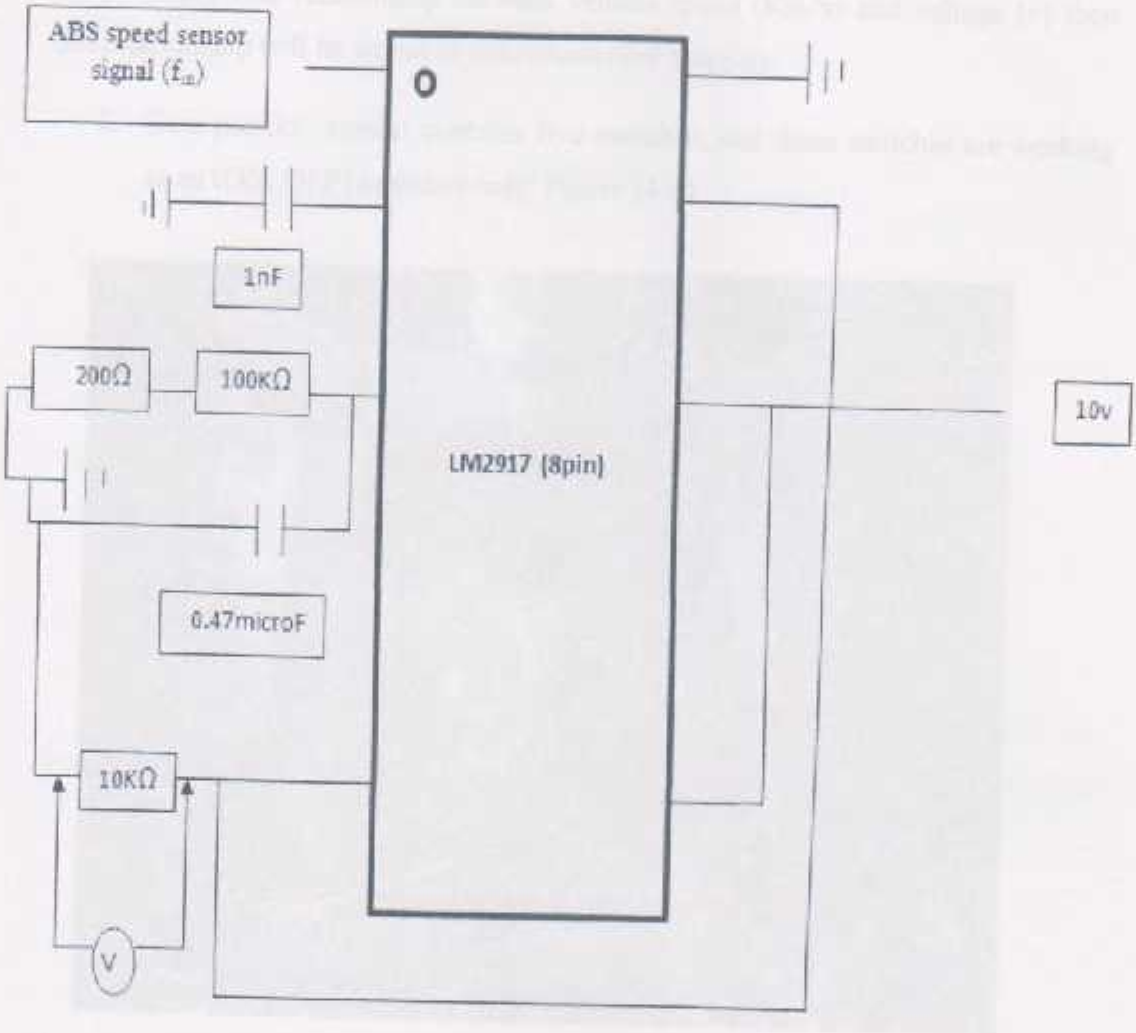

Figure (4-5) Frequency to voltage converter circuit Schematic diagram

This circuit gives linear relationship between frequency and output voltage:

Vout=2*fin   where fin in Khz.   (4.1)

Finally find relationship between vehicle speed (Km/h) and voltage (v) then this relationship will be stored in microcontroller memory.

2. Gear position sensor: contains five switches, and these switches are working as an (ON, OFF) switches only, Figure (4-6).

Figure (4-6) Gear position sensors

Every switch has a circuit which contains: switch, resister - 220 ohm, two batteries 5v, resistance - 100 K ohm, and optocoupler. Optocoupler works as a protection for the signal of the switch circuit, figure (4.7).

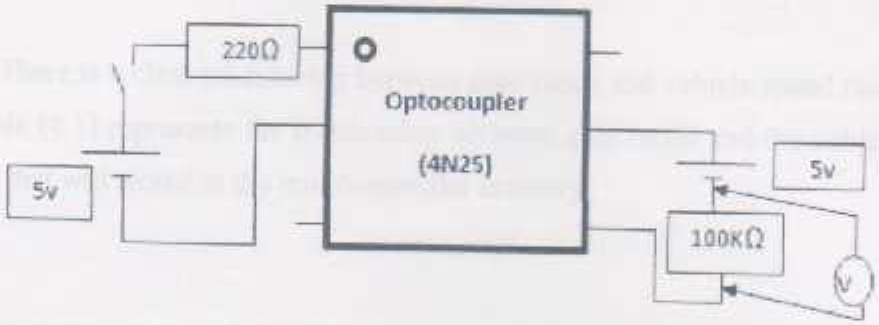

Figure (4-7) Switch circuit Schematic diagram

Switch circuit sends signals direct to microcontroller digital ports without any signal conditioning (amplification, filtration, clamping, converting) is an advantage for the switches, figure (4-8).

Figure (4-8) Path of gear position sensor signals

4.4 Gear ratios and vehicle speed ranges

There is a clear relationship between gear ratios and vehicle speed ranges, and the table (4.1) represents the relationship between gear ratios and the vehicle speed ranges that will stored in the microcontroller memory.

Table (4.1) Gear ratio and the vehicle speed ranges relationship.

Gear Number	Vehicle Speed Range (Km/h)
1	0-20
2	20-40
3	40-60
4	60-140
5	140-200

4.5 Output device

Liquid Crystal Display (LCD) is the output device that display " UP " or "DOWN " when vehicle speed is not suitable with gear number. And it connects directly from microcontroller to take the output signal and show the massage to the driver, figure (4-9) shows the Connection circuit between microcontroller and LCD.

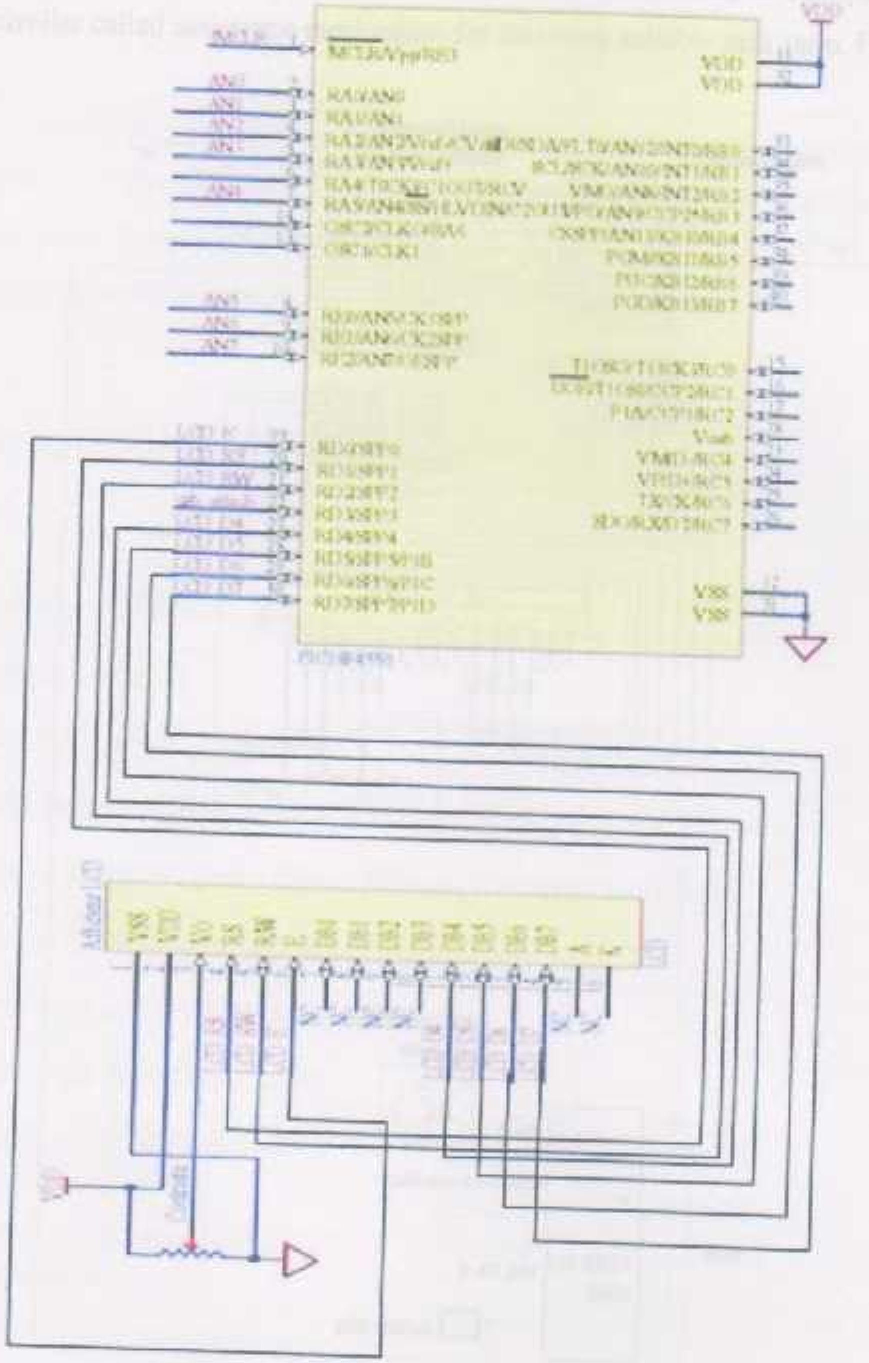

Figure (4-9) Connection circuit between microcontroller and LCD

In the end, we now have an electronic circuit consisting of an input and output controller called assistance mechanism for choosing suitable gear ratio. Figure (4-10)

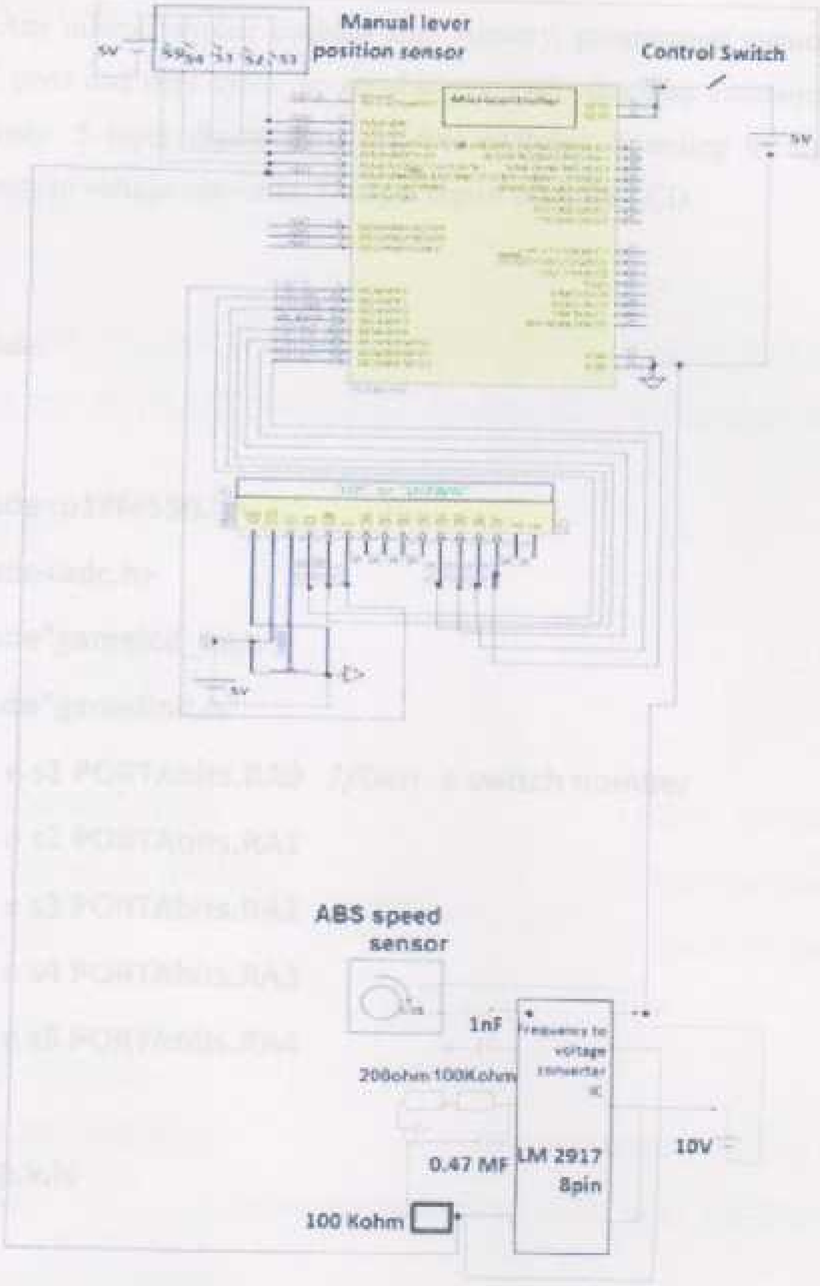

Figure (4-10) Assistance mechanism for choosing suitable gear ratio

4.6 Programming code

Any microcontroller contains user memory, programmer memory, analog to digital ports and duty cycle. So suitable gear ratio choosing assistance mechanism need only: 5 input digital ports for five switches, 1 analog to digital port for frequency to voltage converter, 7 output digital ports for LCD.

The code:

```
#include<p18f4550.h>
#include<adc.h>
#include"gamelcd_v3.h"
#include"gamelinit.h"
#den  e s1 PORTAbits.RA0  //Den  e switch number
#den  e s2 PORTAbits.RA1
#den  e s3 PORTAbits.RA2
#den  e s4 PORTAbits.RA3
#den  e s5 PORTAbits.RA4
{
float sp,v,k;

TRISAbits.TRISA0=1;  //Den  e switch as inputs
TRISAbits.TRISA1=1;
```

```
TRISAbits.TRISA2=1;
TRISAbits.TRISA3=1;
TRISAbits.TRISA4=1;

lcd_init();

OpenADC( ADC_FOSC_8 &ADC_RIGHT_JUST &ADC_4_TAD,ADC_CH0
&ADC_INT_OFF&ADC_VREFPLUS_VDD&ADC_VREFMINUS_VSS,0x0A );

while(1)
{

    ConvertADC();                       // Start conversion
    while(BusyADC());                   // Wait for completion
k=ReadADC();                            // Read result

v=(k*(5/1023));
sp=(59.98*v)+0.0059;                    //calculate the speed
if(s1==1)          //Vehicle Speed range for gear 1(0-20)Km/h
{
if(sp>20)
{
```

```
lcd_gotoyx(1,1);
        lcd_putrs("GEAR UP"); // Display in LCD GEAR UP
WriteCmdXLCD(0x0C) ;

}
}

if(s2==1)           //Vehicle Speed range for gear 2(20-40)Km/h
{
if(sp>40)
{
 lcd_gotoyx(1,1);
        lcd_putrs("GEAR UP"); // Display in LCD GEAR UP
WriteCmdXLCD(0x0C) ;

}
Else
{
if(sp<20)
{
 lcd_gotoyx(1,1);
        lcd_putrs("GEAR DWON"); // Display in LCD GEAR DWON
WriteCmdXLCD(0x0C) ;
```

```
}

}

}

if(s3==1)                    //Vehicle Speed range for gear 3(40-60)Km/h

{

if(sp>60)

{

  lcd_gotoyx(1,1);

            lcd_putrs("GEAR UP"); // Display in LCD GEAR UP

WriteCmdXLCD(0x0C) ;

}

Else

{

if(sp<40)

{

  lcd_gotoyx(1,1);

            lcd_putrs("GEAR DWON"); // Display in LCD GEAR DWON

WriteCmdXLCD(0x0C) ;


}
```

```
}
}
if(s4==1)                    //Vehicle Speed range for gear 4(60-140)Km/h
{
if(sp>140)
{
    lcd_gotoyx(1,1);
            lcd_putrs("GEAR UP"); // Display in LCD GEAR UP
WriteCmdXLCD(0x0C) ;

}
Else
{
if(sp<60)
{
    lcd_gotoyx(1,1);
            lcd_putrs("GEAR DWON"); // Display in LCD GEAR DWON
WriteCmdXLCD(0x0C) ;

}

}
```

```
}
if(s5==1)                    //Vehicle Speed range for gear 5(140-200)Km/h
{
if(sp<140)
{
    lcd_gotoyx(1,1);
            lcd_putrs("GEAR DWON"); // Display in LCD GEAR DWON
WriteCmdXLCD(0x0C) ;


}


}
}
```

Chapter five

Results and recommendations

5.1 Introduction

At the end of this work we can conclude that this project reached it's goal. That to help disable people and new drivers in driving by adding a pneumatic chock absorber on the clutch release mechanism (figure 5-1) to prevent engine stalling during vehicle takeoff, and adding LCD on the dash board (figure 5-2) to warn the driver if he didn't choose the proper gear ratio which match the vehicles speed by showing a massage " gear up" or " gear down" This means that the driver should shift up or shift down the gear ratio.

Figure (5-1) pneumatic - chock - absorber on clutch pedal

Figure (5-2) LCD to warn driver to shift up or shift down gear ratio

Through the above mentioned we came out with a set of results as well as some of the recommendations that would improve the efficiency of the work of the mechanical mechanism and electrical system.

5.2 Result

The results of this project can be summarized as follows: -

1- The disabled people can be driving cars with manual gearbox.

2- Engine that does not stop working suddenly; helps to keep the brake system in action.

3- Engine that does not stop working suddenly; helps to reduce accidents

4- Engine that does not stop working suddenly helps to reduce traffic congestion, especially in cities.

5- Engine that does not stop working suddenly leads to reduce fuel consumption, since the process engine to stop and restart the need to start each time to more fuel.

6- Easily and quickly training driver on leadership, at this assistance mechanisms in vehicle.

7- Avoid the shock in the clutch system lead to increase working life, through maintaining internal parts.

5.3 Recommendations

And also at the end of this project, and know the Strengths and weaknesses point of it, we have developed some recommendations like:

1- Speaker supplying the electrical system, to warn the driver through the hearing to ensure that the driver knows the warning.

2- Use one Sensor to identify the gear position instead five switches.

3- Installing - chock - absorber in front of vehicle instead of the driver's compartment to ensure that no dust and dirt enter into - chock - absorber.

4- To provide the electrical system voltage appropriate of vehicle battery.

5- Use software that contains the direct transfer of frequency to voltage without the need for electronic part for the same purpose.

References:

[1] http://en.wikipedia.org/wiki/Shock_absorber

[2] Heinz Heisler, Advanced vehicle technology, second edition, page 60, 2002.

[3] Tom Denton, Automobile electrical and electronic systems, third edition, page 38, 2004.

[4] Tom Denton, Advanced automotive fault diagnosis, second edition, page 40, 2006.

[5] Improving boost pressure response of turbocharged diesel engines, first edition, page 20, 2012.

[6] Norman S. Nise, Control systems engineering, sixth edition, page 172, 2011.

[7] Singiresu S. Rao, Mechanical vibrations, third edition, 1995.

[8] J. Giacomin, Measurement of the comfort of automobile clutch pedal actuation.

APPENDIX

VISHAY.

Optocoupler, Phototransistor Output, with Base Connection

21842

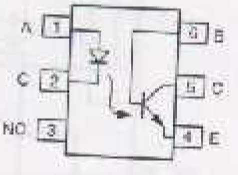

FEATURES

- Isolation test voltage 5000 V_{RMS}
- Interfaces with common logic families
- Input-output coupling capacitance < 0.5 pF
- Industry standard dual-in-line 6 pin package
- Compliant to RoHS directive 2002/95/EC and in accordance to WEEE 2002/96/EC

RoHS COMPLIANT

APPLICATIONS

- AC mains detection
- Reed relay driving
- Switch mode power supply feedback
- Telephone ring detection
- Logic ground isolation
- Logic coupling with high frequency noise rejection

AGENCY APPROVALS

- UL1577, file no. E52744
- BSI: EN 60065:2002, EN 60950:2000
- FIMKO: EN 60950, EN 60065, EN 60335

DESCRIPTION

The 4N25 family is an industry standard single channel phototransistor coupler. This family includes the 4N25, 4N26, 4N27, 4N28. Each optocoupler consists of gallium arsenide infrared LED and a silicon NPN phototransistor.

ORDER INFORMATION	
PART	REMARKS
4N25	CTR > 20 %, DIP-6
4N26	CTR > 20 %, DIP-6
4N27	CTR > 10 %, DIP-6
4N28	CTR > 10 %, DIP-6

ABSOLUTE MAXIMUM RATINGS (1)				
PARAMETER	TEST CONDITION	SYMBOL	VALUE	UNIT
INPUT				
Reverse voltage		V_R	5	V
Forward current		I_F	50	mA
Surge current	t ≤ 10 µs	I_{FSM}	3	A
Power dissipation		P_{diss}	100	mW
OUTPUT				
Collector emitter breakdown voltage		V_{CEO}	70	V
Emitter base breakdown voltage		V_{EBO}	7	V
Collector current		I_C	50	mA
	t < 1 ms	I_C	100	mA
Power dissipation		P_{diss}	150	mW

Typical Applications (Continued)

Changing the Output Voltage for an Input Frequency of Zero

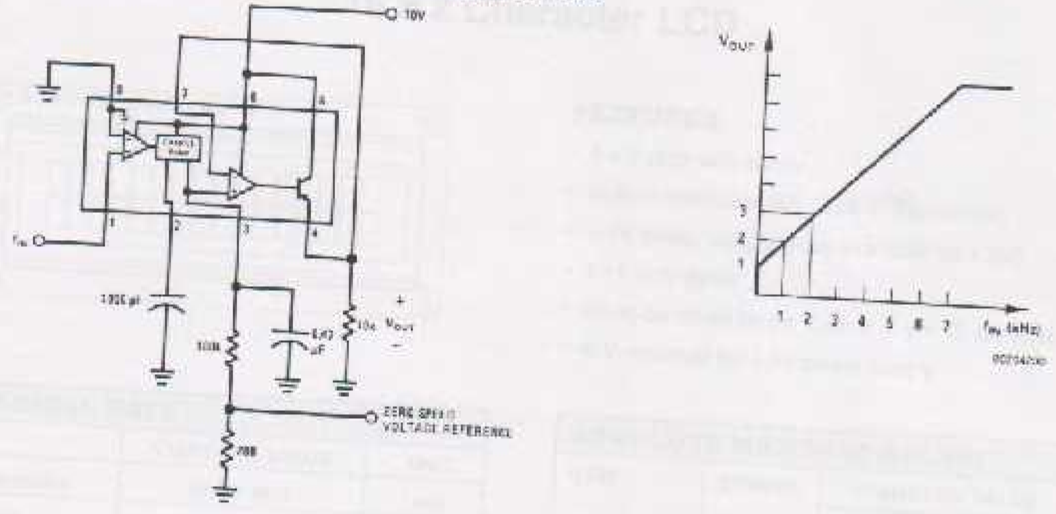

Changing Tachometer Gain Curve or Clamping the Minimum Output Voltage

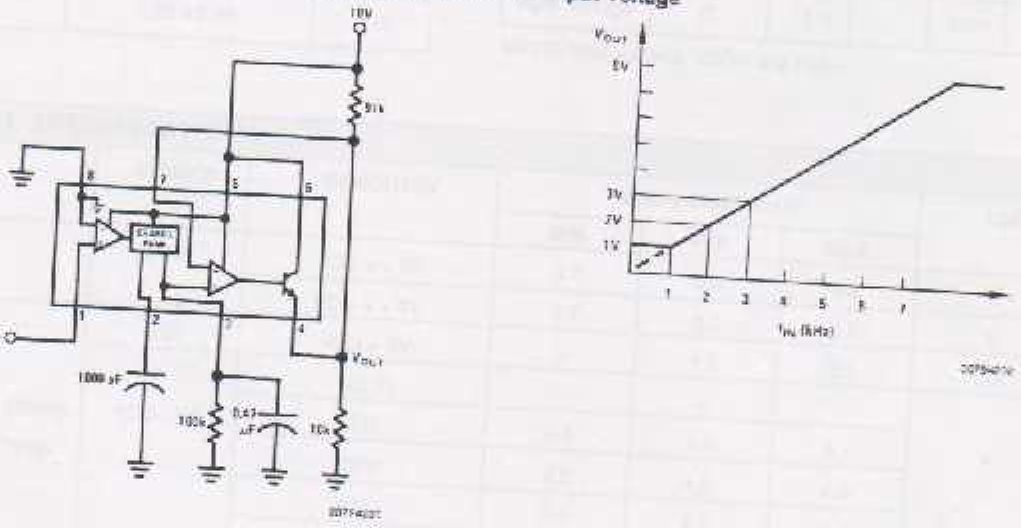

16 x 2 Character LCD

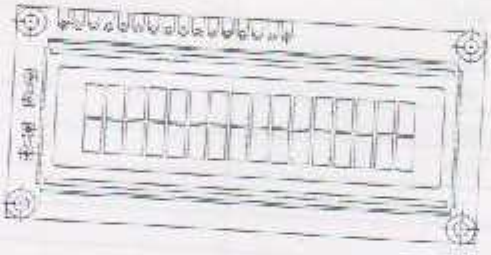

FEATURES

- 5 x 8 dots with cursor
- Built-in controller (KS 0066 or Equivalent)
- + 5V power supply (Also available for + 3V)
- 1/16 duty cycle
- B/L to be driven by pin 1, pin 2 or pin 15, pin 16 or A.K (LED)
- N.V. optional for + 3V power supply

MECHANICAL DATA

ITEM	STANDARD VALUE	UNIT
Module Dimension	80.0 x 36.0	mm
Viewing Area	66.0 x 16.0	mm
Dot Size	0.56 x 0.66	mm
Character Size	2.96 x 5.56	mm

ABSOLUTE MAXIMUM RATING

ITEM	SYMBOL	STANDARD VALUE			UNIT
		MIN.	TYP.	MAX.	
Power Supply	VDD-VSS	- 0.3	–	7.0	V
Input Voltage	VI	- 0.3	–	VDD	V

NOTE: VSS = 0 Volt, VDD = 5.0 Volt

ELECTRICAL SPECIFICATIONS

ITEM	SYMBOL	CONDITION		STANDARD VALUE			UNIT
				MIN.	TYP.	MAX.	
Input Voltage	VDD	VDD = + 5V		4.7	5.0	5.3	V
		VDD = + 3V		2.7	3.0	5.3	V
Supply Current	IDD	VDD = 5V		–	1.2	3.0	mA
Recommended LC Driving Voltage for Normal Temp. Version Module	VDD - V0	- 20 °C		–	–	–	V
		0°C		4.2	4.8	5.1	
		25°C		3.8	4.2	4.6	
		50°C		3.6	4.0	4.4	
		70°C		–	–	–	
LED Forward Voltage	VF	25°C		–	4.2	4.6	V
LED Forward Current	IF	25°C	Array	–	130	260	mA
			Edge	–	20	40	
EL Power Supply Current	IEL	Vel = 110VAC:400Hz		–	–	5.0	mA

DISPLAY CHARACTER ADDRESS CODE:

Display Position

	1	2	3	4	5	6	7	8	9	10	11	12	13	14	15	16
DD RAM Address	00	01														0F
DD RAM Address	40	41														4F

LCD-016M002B

Vishay

16 x 2 Character LCD

PIN NUMBER	SYMBOL	FUNCTION
1	Vss	GND
2	Vdd	+ 3V or + 5V
3	Vo	Contrast Adjustment
4	RS	H/L Register Select Signal
5	R/W̄	H/L Read/Write Signal
6	E	H →L Enable Signal
7	DB0	H/L Data Bus Line
8	DB1	H/L Data Bus Line
9	DB2	H/L Data Bus Line
10	DB3	H/L Data Bus Line
11	DB4	H/L Data Bus Line
12	DB5	H/L Data Bus Line
13	DB6	H/L Data Bus Line
14	DB7	H/L Data Bus Line
15	A/Vee	+ 4.2V for LED/Negative Voltage Output
16	K	Power Supply for B/L (OV)

DIMENSIONS in millimeters

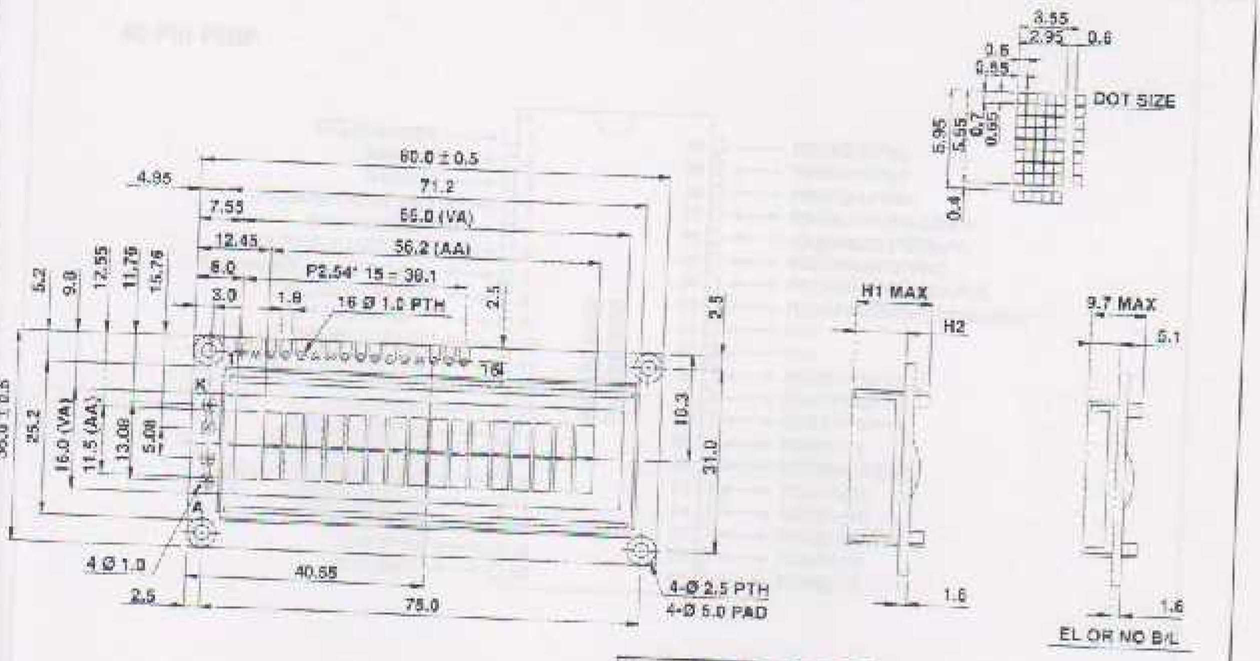

LED - H/L B/L	HIGH	LOW
H1	13.2	12.1
H2	8.6	7.5

Pin Diagrams

28-Pin PDIP, SOIC

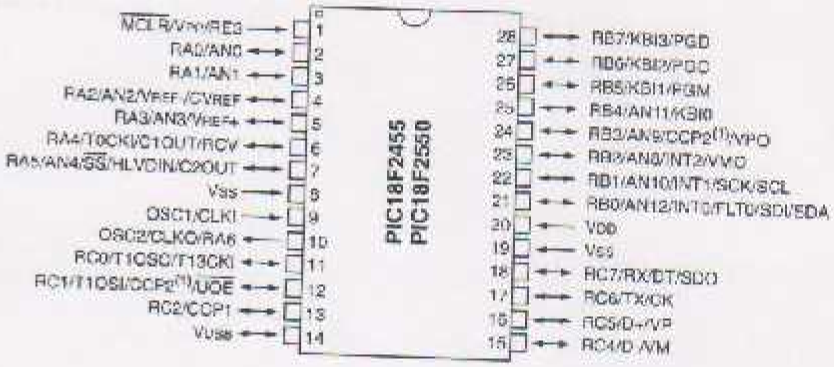

40-Pin PDIP

Note 1: RB3 is the alternate pin for CCP2 multiplexing.